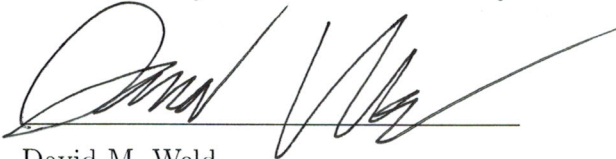


# Synthesis and Characterization of Stochastically Nanostructured Metallic Films

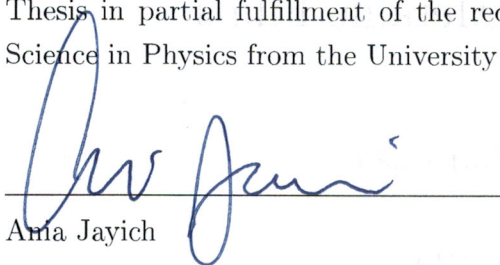
Alexander Kotlerman

I certify that this dissertation fulfills the requirements for the Bachelor's Honors Thesis in partial fulfillment of the requirements for the degree of Bachelor of Science in Physics from the University of California, Santa Barbara.

A handwritten signature in black ink, appearing to read "David M. Weld", written over a horizontal line.

David M. Weld  
(Principal Adviser)

I certify that this dissertation fulfills the requirements for the Bachelor's Honors Thesis in partial fulfillment of the requirements for the degree of Bachelor of Science in Physics from the University of California, Santa Barbara.

A handwritten signature in blue ink, appearing to read "Anna Jayich", written over a horizontal line.

Anna Jayich

# Abstract

Thermal evaporation in a high background pressure is capable of producing nanostructure films. These nanostructured films, dubbed metal blacks, are easy to synthesize. Highly nanostructured materials appear black and have intrinsically low reflectivity. This property enables possible applications for detection of light. We describe the development of synthesis techniques for nanostructured Cu, Al, Ag, Au, Mg, Cr, Bi, and Fe. These elements were found to have varying degrees of blackness and structure based on method of evaporation. We also present initial characterization measurements of the films physics, optical, electrical, and photoacoustic properties.

# Acknowledgements

For my mother and family

I would like to thank Professor David Weld for advising me on this thesis. He will forever be ingrained as one of the most influential people in my life for uniquely contributing to my growth as a person. I also give thanks to the members of the Weld group, Erica, Anne, Eric, Max, Zak, Ruwan, Shankari, Slava, Kurt, and Robert who I now cherish and love as friends. We grew intellectually and matured together in the lab. The time spent bonding over our physics studies is something of great personal value. A special thanks to Erica for showing me what it actually means to work hard and love work and Slava for his unquenchable thirst to answer questions and solve problems. It would not have been possible for me to complete my duties in the lab and as a physics student without the inspiration these people have given me.



# Contents

<b>1</b>	<b>Introduction</b>	<b>7</b>
1.1	Motivations . . . . .	7
<b>2</b>	<b>Experimental setup and Synthesis</b>	<b>7</b>
2.1	Preliminary Theory and Calculations . . . . .	7
2.1.1	Simulating DLA . . . . .	7
2.1.2	Fractal dimension of three dimensional DLA . . . . .	8
2.1.3	Mean Free Path . . . . .	9
2.1.4	Vapor Pressure . . . . .	10
2.1.5	Deposition Rate . . . . .	11
2.1.6	Temperature . . . . .	11
2.1.7	Boat Temperature . . . . .	12
2.1.8	Pumping Considerations . . . . .	13
2.2	Synopsis of Work . . . . .	14
2.3	Setup . . . . .	15
2.3.1	First setup, stock . . . . .	16
2.3.2	Second setup, elevated boat . . . . .	16
2.3.3	Third setup . . . . .	16
2.3.4	Fourth setup . . . . .	17
2.3.5	Zeroth setup: no substrate holder or cooling . . . . .	18
2.4	Observations and Resulting Films . . . . .	18
2.4.1	Copper . . . . .	19
2.4.2	Silver . . . . .	19
2.4.3	Aluminum . . . . .	20
2.4.4	Iron . . . . .	20
2.4.5	Chromium . . . . .	21
2.4.6	Gold . . . . .	21
2.4.7	Indium . . . . .	21
2.4.8	Magnesium . . . . .	22
2.5	Vacuum sensors and controller . . . . .	22
<b>3</b>	<b>Morphology</b>	<b>23</b>
3.1	SEM results . . . . .	23
3.2	Assumptions based on SEM results . . . . .	26
<b>4</b>	<b>Optical Properties</b>	<b>26</b>
4.1	Reflectometry . . . . .	27
<b>5</b>	<b>Photoacoustic Properties</b>	<b>27</b>
5.1	Theory . . . . .	29
5.2	Experimental Setup . . . . .	29
5.3	Results and correlation to theory . . . . .	33
5.4	Acoustic Phased Array . . . . .	34

<b>6 Conclusion</b>	<b>35</b>
6.1 Avenues of further research . . . . .	35
<b>Appendices</b>	<b>37</b>
<b>A Mathematica Code</b>	<b>37</b>
A.1 Photoacoustic Simulation . . . . .	37
A.2 Computing Fractal Dimension . . . . .	37
<b>B Python code</b>	<b>38</b>
B.1 Generate DLA . . . . .	38
<b>C Evaporation Notes</b>	<b>41</b>
C.1 6/09/12, Cu-black . . . . .	41
C.2 7/03/12, Cu-black . . . . .	42
C.3 7/11/12, Cu-black . . . . .	42
C.4 7/12/12, In-black . . . . .	42
C.5 7/13/12, In-black . . . . .	43
C.6 7/13/12, Al-black . . . . .	43
C.7 7/17/12, Al-black . . . . .	44
C.8 7/17/12, Al-black . . . . .	44
C.9 7/17/12, In-black . . . . .	45
C.10 7/17/12, Cu-black . . . . .	45
C.11 7/19/12, Cu-black . . . . .	46
C.12 7/19/12, Al-black . . . . .	46
C.13 7/19/12, Cu-black . . . . .	46
C.14 7/20/12, Cu-black . . . . .	47
C.15 7/23/12, Al-black . . . . .	47
C.16 7/23/12, Al-black . . . . .	47
C.17 7/24/13, In-black . . . . .	48
C.18 7/25/12, In-black . . . . .	48
C.19 8/03/12, Al-black . . . . .	48
C.20 8/03/12, Al-black . . . . .	49
C.21 8/06/12, In-black . . . . .	49
C.22 8/06/12, Al-black . . . . .	49
C.23 8/07/12, Sn-black . . . . .	50
C.24 8/08/12, Cu-black . . . . .	50
C.25 8/09/12, Mg-black . . . . .	50
C.26 8/24/12, Cr-black . . . . .	51
C.27 8/31/12, Au-black . . . . .	51
C.28 9/06/12, Fe-black . . . . .	52
C.29 9/10/12, Fe-black . . . . .	52
C.30 2/14/13, Cu-black . . . . .	53
C.31 4/05/13, Cu-black . . . . .	53
C.32 4/15/13, Cu-black . . . . .	54

C.33 4/29/13, Cu-black . . . . .	54
C.34 5/03/13, Sn-black . . . . .	54

**D Photoacoustic data** **55**

**List of Figures**

1	DLA simulations . . . . .	8
2	Water cooling setups of the evaporator . . . . .	15
3	Zeroth setup: Hanging Copper Foil . . . . .	18
4	True vs Measured pressure in different gases for 275 type convectron gauge[1]	22
5	Comparison between simulated and metal black DLA . . . . .	23
6	SEM images of Silver and Indium at different scales . . . . .	24
7	Some interesting SEM images . . . . .	25
8	Gray Silver, Black silver, and Black copper side-by-side at 20000x magnification	25
9	Nanostructured Aluminum . . . . .	26
10	Reflectometry results . . . . .	28
11	Circuits used in the photoacoustic experiment . . . . .	30
12	SPU0410LR5H MEMs microphone response with respect to frequency . . . .	32
13	Unusable frequency versus amplitude measurements dominated by electrical coupling . . . . .	33
14	Focused photoacoustic intensity using planoconcave lens . . . . .	34

# 1 Introduction

## 1.1 Motivations

In the last century it has become common knowledge that changing the structure of a material can often lead to changes in the intrinsic properties of a material. Metal blacks have been known to be associated with a decrease in reflectivity which make them suitable for light detection. Well known evaporation techniques [4] coupled with initial speculation for the uses of metal blacks for IR sensors [8] established initial speculation on the properties of metal blacks. Using DLA (diffusion limited aggregation) simulations it can be shown that the nanostructure of metal blacks is essentially element independent. Different metals, commonly silver [12] and gold, were determined to be metal black candidates and further supported the claim that other metals can also produce nanostructured films. Combined with the availability of a variety of cheap high purity metals the project started to test as many elements as possible.

## 2 Experimental setup and Synthesis

### 2.1 Preliminary Theory and Calculations

Stochastic nanostructure depends on random events that take place on the atomic to micrometer scale. Diffusion Limited Aggregation (DLA) is the process by which particles undergoing Brownian motion (random collision with neighboring particles) grow into structures. Particles in the evaporator are assumed to undergo a random walk due to constant bombardment with argon gas molecules. Encounters with other particles cause them to “stick” and form clumps which, in turn, continue to grow in the same fashion. Simulations for a random walk are easy to create and quantifying the structure can be achieved by calculating the fractal dimension, a number describing the statistical complexity of a geometric pattern.

#### 2.1.1 Simulating DLA

Python code to generate DLA is found in Appendix B.1. DLA is generated by randomly generating a particle on a circle of radius  $r$  determined to be far enough to come from “infinity” but, at the same time, reduce processing time to the smallest value possible. Generated particles randomly walk either left, right, up, or down until they are either outside a set boundary or hit another particle.

Fractal dimensions are good numbers to use to determine the scaling describing the structure of materials created under stochastic processes. They describe the detail of a pattern as a function of scale. Fractal dimensions are subsequently calculated empirically by

$$\frac{\log N(\varepsilon)}{\log(1/\varepsilon)}$$

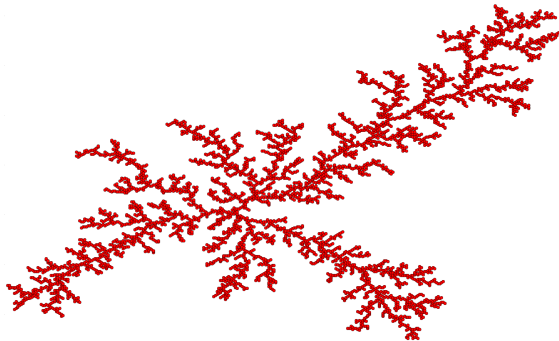
where  $N(\varepsilon)$  is the number of boxes of length  $\varepsilon$  necessary to cover an edge of a pattern as derived from the power law relation  $N(\varepsilon) = (1/\varepsilon)^D$ . More edges correspond to a higher  $N(\varepsilon)$  but to see those edges requires a lower  $\varepsilon$ . Plotting  $N(\varepsilon)$  vs  $1/\varepsilon$  under a log-log scale produces a straight line with slope defined as the fractal dimension as given above. For a diffusion limited aggregate in a two dimensional plot a typical value is about 1.71.

One method to determine a fractal dimension is to use box counting. Box counting partitions a binarized (two possible values for each pixel) image followed by tracing the edge of the image. All partitioned segments that are not black are counted. The size of each box is arbitrarily chosen based on desired simulation speed and accuracy. Box count is plotted and the fractal dimension recorded. Mathematica code to obtain the fractal dimension is located in Appendix A.2.

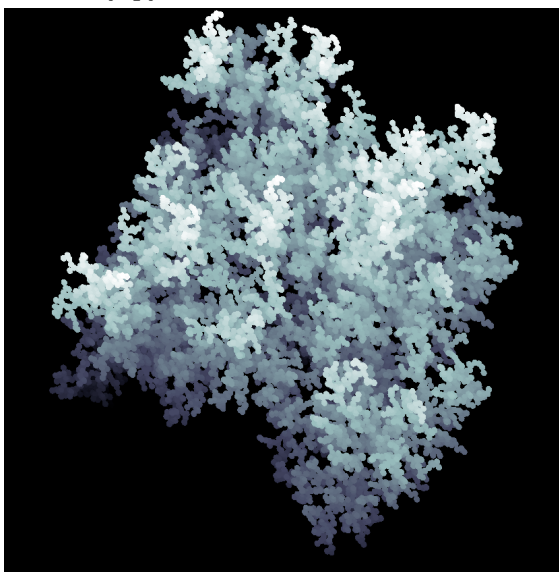
Four DLA's were generated in parallel consisting of 5000 particles each and the fractal dimension is measured on each one using mathematica code from Appendix A.2. Each image looks roughly like Figure 1a. Measured fractal dimensions are: 1.692, 1.754, 1.680, 1.685. These four sample have an error 1.7% from the actual value of 1.71.

### 2.1.2 Fractal dimension of three dimensional DLA

SEM images above show a three dimensional structure. Results of simulations of three dimensional DLA are shown in Figure 1b. Finding the fractal dimension for these systems



(a) 2D DLA composed of 5000 particles generated by python code



(b) 3D DLA composed of 3000 particles generated by python code

Figure 1: DLA simulations

is much more difficult, especially using SEM's where only one angle of an object is visible. Nevertheless it is still possible by taking two dimensional slices of the SEM images the fractal dimension can be measured and interpreted. Fractal dimension of real samples will reflect the contrast and clarity of the picture. When applying binarization to the images many shadows and other features will also appear and be taken into account. Such extra features will artificially increase the fractal dimension of the image. To combat this effect other fractal dimension measurement techniques would need to be applied. Other possibilities include omitting data that is not an "edge" to the image.

### 2.1.3 Mean Free Path

Thermal deposition is a common technique for synthesizing films. By using high resistivity boats made of a metal with low vapor pressure (such as tungsten and molybdenum) different metals are evaporated under vacuum. When the metal is heated the vapor pressure is increased substantially. Under vacuum the vapor's mean free path increases and allows the vapor metal to travel and adhere to a substrate in solid form. This process is called deposition.

Under normal thermal evaporation materials are deposited in high vacuum onto a substrate far enough such that an even distribution of material will be deposited. High vacuum must correspond to a mean free path equal or larger than the source to substrate distance. Such evaporations require that each atom is deposited evenly and predictably.

Metal blacks require deposition to be performed at low vacuum on the order of 1 Torr to appear black. Separate research by Harris [4] and Lehman [8] shows that the quality of metal black films rely on many contributing factors dependent on the evaporator setup. Deposition parameters by Harris and Lehman are compared to the parameters used in this experiment. Due to differences in configuration many of the derived parameters for metal black depositions are unique to this thesis.

Water cooling and substrate distance are found to have the highest correlation to good black films. The mean free path for kinetic gases (modeled as points) is

$$\lambda = \frac{k_B T}{\sqrt{2} \pi d^2 P} \quad \text{where}$$

$k_B$	Boltzmann Constant
$T$	Temperature in Kelvin
$d$	Diameter of particles
$P$	Pressure in Pa

As pressure decreases the mean free path increases due to fewer collision with the surrounding gas. The substrate distance to the source therefore determines the time of deposition and

deposition rate. The Knudsen number,  $Kn = \lambda/L$  (where L is the substrate distance) determines the regime of the process: either high vacuum ( $Kn > 1$ ) or fluid-flow ( $Kn < 1$ ). Due to the low vacuum this experiments works in the regime of fluid-flow with  $Kn = \lambda/L \approx 1\mu m/10cm \ll 1$ . Fluids are therefore best approximation for the behavior of the particles during the deposition process.

#### 2.1.4 Vapor Pressure

The vapor pressure of a given liquid or solid changes when in a vacuum and determines the deposition rate during thermal deposition. The vapor pressure can be determined by equating the chemical potentials of liquid and gas and using the ideal gas law:

$$\mu_l^\circ = \mu_g^\circ$$

$$\text{Constant volume liquid with external pressure: } \Delta\mu_l = \left(\frac{V}{n}\right) (P_{ext} - P_{ref})$$

$$\text{Non constant volume gas: } \Delta\mu_g = \int \frac{V}{n} dP = RT \int \frac{dP}{P} = RT \ln \frac{P_v}{P_{v,ref}}$$

$$\left(\frac{V}{n}\right) (P_{ext} - P_{ref}) = RT \ln \frac{P_v}{P_{v,ref}}$$

$$P_{vapor} = P_{v,ref} \exp \left[ \frac{V}{nRT} (P_{ext} - P_{ref}) \right]$$

Where  $P_{ref}$  is the reference pressure and  $P_{v,ref}$  is the vapor pressure at the reference pressure.

To find the vapor pressure at atmospheric pressure for liquid copper the Clausius-Clapeyron Equation can be used. At 2420K copper (melting point 1358K) has an enthalpy of vaporization of 304.6kJ/mol at atmospheric pressure, a reference pressure  $P_2 = 5$  kPa at 2320 leaves the value of:

$$\ln \frac{P_1}{P_2} = \frac{H_{vap}}{R} \left( \frac{1}{T_2} - \frac{1}{T_1} \right)$$

$$P_1 = 9.6 \text{ kPa}$$

The real value of 10 kPa[6] (error  $\approx 4\%$ ) is close enough to the calculated value that the Clausius-Clapeyron Equation can be successfully use to determine the vapor pressure for a known temperature. Similar arguments are used for all the other metals used in this thesis.

For the vapor pressure under vacuum, at 1 Torr (0.00132atm) the equation for vapor pressure is used above. Applying the missing variable, the molar volume of copper  $V/n = 7.0920cm^3/mol$ , the result is the same within 1%. As a result the only relevant formula

to determine the deposition rate is the Clausius-Clapeyron equation. In other words the deposition rate is about the same between low vacuum and room pressure.

### 2.1.5 Deposition Rate

Under normal deposition the vacuum pressure is in the high vacuum region ( $10^{-6}$  Torr to  $10^{-8}$  Torr). For depositions under high vacuum, where  $K_n > 1$ , a quartz crystal monitor is used. Quartz crystal monitors are often used to find the rate of deposition by measuring changes in resonance frequency of a crystal as material is deposited. In this scenario a quartz crystal monitor would be useless as the deposition rate changes drastically depending on distance as explained below.

In the fluid-flow regime, deposition rate depends on three main factors: temperature, pressure, and distance. Source-to-substrate distance determines the deposition rate in a fluid system via the mean free path (which, in turn, is determined by the pressure). If the mean free path of a particle is small the number of collision before hitting a far-away substrate will be large. Consequently the probability of a particle hitting the substrate decreases. On average a particle has a higher probability of hitting a substrate that is within line-of-sight. A particle is unlikely to go around an obstacle without the help of some current (this is experimentally verified: very little metal black appears on surfaces that are not line-of-sight). Therefore the probability of hitting a substrate for a short mean free path will be determined by the solid angle of the source and size of the substrate. In the evaporator a standard boat used is the R. D. Mathis S2B type. S2B model boats have a small spherical dimple 1/8" deep allowing for large solid angles.

Thicker films are created by either increasing the deposition time or increasing the vapor pressure. Synthesizing metal blacks require a vapor pressure between 100 mTorr and 10 Torr.

### 2.1.6 Temperature

As the temperature of the boat rises heat is diffused into the surrounding inert gas (such as Argon). The rising temperature also causes the boat to radiate in the fashion of a blackbody. At 2000K the blackbody radiation released is given by the Stephen-Boltzmann law (with emissivity of  $\epsilon \approx 0.05$ )  $j \approx \epsilon \sigma T^4 = 45 \text{ kW/m}^2$  at the surface of the evaporant. This is a large amount of radiation and actively changes the results of the deposition. Measurements on the copper substrate used in this thesis (discussed later) show that the reflectivity is, very roughly,  $60\% \pm 10\%$  across the spectrum measured. This means at the beginning of the deposition 40% of incident light is absorbed. Roughly measuring the flux to be



1% of the total radiation on the film and assuming perfect vacuum the substrate absorbs  $5\% \times 40\% \times 45000 W/m^2 \times 4\pi(0.05m)^2 \approx 30 W$ .

Cooling by the surrounding inert gas also plays a role. The heat flux can be expressed as

$$\Phi = \frac{K_T}{b} (T_h - T_s) \quad \text{where} \quad \begin{array}{l|l} K_T & \text{Thermal conductivity} \\ b & \text{Gap length} \end{array}$$

For Argon,  $K_T \approx 0.018 Wm^{-1}K^{-1}$ , and letting  $b \approx 5 cm$ , then a Copper substrate at  $298K$  receives a flux of  $\approx \epsilon 600 W/m^2 = 20 mW$ . The equilibrium temperature without any cooling is reached when the heat dissipated by the surrounding gas is the same as the heat absorbed by the film. The calculations for this process is more complicated because of the dark (anti-reflective) and porous properties of the films produced. A larger amount of metal black deposited corresponds to a lower reflectance and a increase in the heating of the sample. Further issues include low thermal conductivity with the substrate due to porosity.

With time the heat transfer to argon increases the temperature and consequentially expands. As the gas expands it starts to increase the pressure of the system. Increasing pressure decreases the mean free path and in order to retain a steady state periodic pump-downs are required.

### 2.1.7 Boat Temperature

Boat temperature is an important aspect of deposition. The rate of particles leaving the boat directly determines the rate of film growth (assuming constant pressure). To find the real temperature of the boat to a high precision is difficult. Predicting the temperature theoretically is also problematic. Low vacuum and copper leads securing the boat source are both sources of thermal conduction. As the boat source gets hotter heat transfers into colliding gas particles and leaks into the copper leads, complicating theoretical predictions of the temperature. However, an attempt can be made to compensate for fluctuations in temperature.

Joule heating is responsible for the temperature of the boat. Applying the Stephen-Boltzmann law in the case where the net power is

$$P_{net} = P_{emit} - P_{absorb}$$

$$P_{net} = A\sigma\varepsilon(T^4 - T_0^4) \quad \text{where}$$

$\sigma$	Stephen-Boltzmann Constant
$A$	Surface Area
$T$	Temperature of boat
$T_0$	Temperature of surrounding gas
$\varepsilon$	Absorbitivity

Order of magnitude calculations can determine how fast the current has to be increased in order to maintain a specific heat. The resistance with respect to temperature of some relevant metals are given by

$$R = R_{ref} [1 + \alpha (T - T_{ref})] \quad \text{where}$$

$\alpha_W$	$0.004403 \text{ } ^\circ\text{C}^{-1}$
$\alpha_{Mo}$	$0.004579 \text{ } ^\circ\text{C}^{-1}$
$\alpha_{Cu}$	$0.004290 \text{ } ^\circ\text{C}^{-1}$

and the emitted power is given by

$$P = I^2 R$$

These formulas prove that it is possible to roughly measure the temperature simply measuring the area of the boat, the voltage drop across the boat, and the current.

### 2.1.8 Pumping Considerations

When the temperature of the inert gas increases the pressure also increases. At 5 Torr an increase of  $50^\circ\text{C}$  from room temperature for an ideal gas corresponds to a new pressure

$$P_1 = T_1 \frac{P_0}{T_0} = 348K \frac{5T}{298K} = 5.84\text{Torr}$$

$$\Delta P = 0.8\text{Torr}$$

The mean free path change can be found by:

$$\frac{\lambda_1 P_1}{T_1} = \frac{\lambda_2 P_2}{T_2}$$

$$\lambda_1 = 9.450\text{mm} \quad \lambda_2 = 9.448\text{mm} \quad \Delta\lambda = 2\mu\text{m}$$

Due to the low change in mean free path temperature can effectively be ignored. Changes in pressure, on the other hand, produce a large change in mean free path. If the pressure increases from 1 Torr to 5 Torr the mean free path decreases by a factor of 5.

## 2.2 Synopsis of Work

The first goal had been to make the indium evaporator operational. Using materials from R. D. Mathis Company and an old belt pump the system was installed and its condition verified. Issues that hindered accurate depositions include a broken ion gauge, non-automated gate control, and no on-board computer. A working diffusion pump came with the system which allowed the system to reach high vacuum although it was impossible to determine how low the pressure will go. Miscellaneous work involved taking apart the vacuum plumbing in order to clean each junction and guarantee a vacuum seal.

A Welch 1397 belt pump is included with the setup designed to achieve pressures below 30 mTorr. Initially the pump would not go under 50mTorr. Flushing the pump fixed the issue and allowed for roughing pressures as low as 25mTorr as well as ensuring long-term use. 8 feet of Gum Rubber tubing with a 1 inch diameter was used to connect the pump to the evaporator. About 1500 cubic inches is evacuated by the pump.

Boats were chosen based on the evaporator configuration and source material. Lists of metals, evaporation type, recommended boats, and vapor pressures were used in order to choose the right boat for the right job (See [http://www.lesker.com/newweb/deposition\\_materials/MaterialDeposition.cfm](http://www.lesker.com/newweb/deposition_materials/MaterialDeposition.cfm)).

Metal black films were deposited using thermal deposition onto various substrates using tungsten and molybdenum boats with and without cooling. Techniques and methods of evaporation were tested, analyzed, and discussed. Substrates used include glass, copper foil, and mica. Results were observed and the deposition parameters were changed accordingly until the darkest film was produced. Although initial samples were not black trial and error resulted in two modifications to the evaporator in an attempt to achieve the blackest results possible. Four configurations were used to evaporate the films and basic maintenance and cleanup was done periodically due to the residue left over from sequential evaporations.

Reflectometry, photoacoustic, and SEM measurements of metal black films were taken and results were compared to previous research on metal blacks [4]. SEM measurements at CNSI were taken and produced results for eight different metal black samples. Reflectometry measurements using machinery at the MRL TEMPO facility were also done on various samples. Measurements from these facilities were analyzed and discussed. Further characterization involved a photoacoustic experiment. Two circuits were built for the experiment: one for driving a high powered LED and one for driving a high frequency microphone. These circuits were used to attempt to determine the frequency vs. amplitude response of the films.

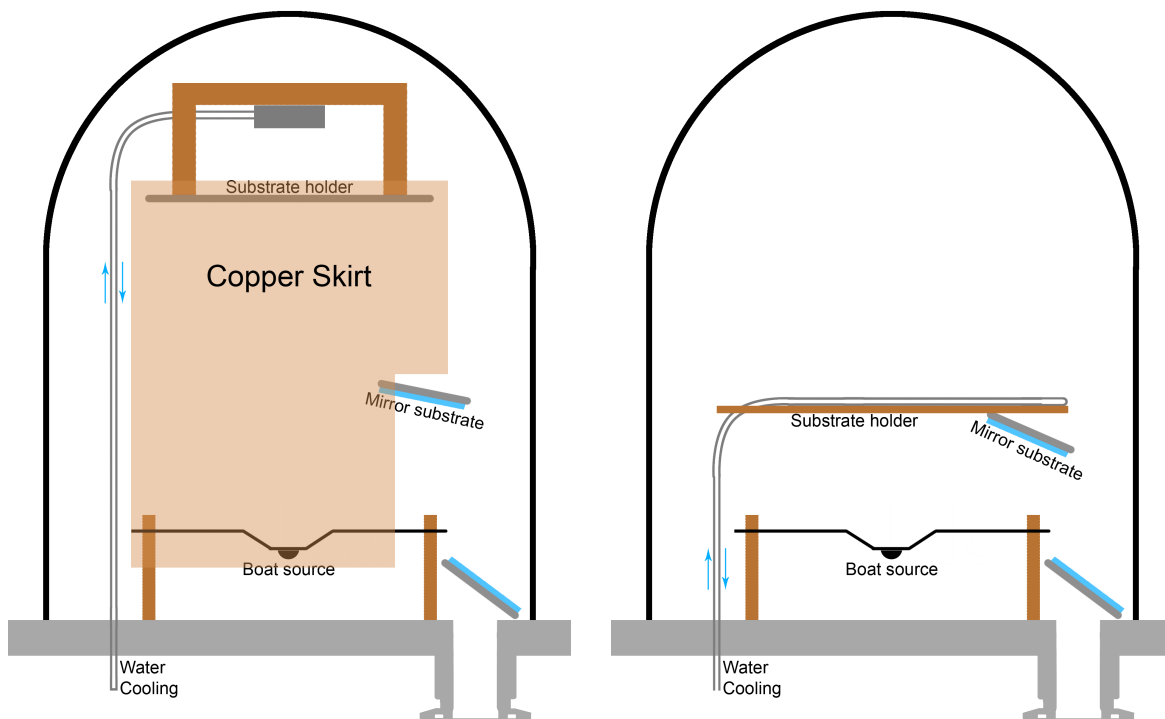
Other research involved finding applications for the films. For example acoustic phased arrays, utilizing the photoacoustic effect [2], could provide a cheap alternative to common

ultrasound technology.

## 2.3 Setup

The degrees of freedom present in our evaporator are the substrate distance, cooling method, pressure, and current through the boat. There have always been at least two places for substrates: one on the top plate and another as the mirror looking into the boat (see Figure 2). Other substrates include aluminum foil covering components throughout the evaporation chamber. Samples are labeled, stored, and analyzed. Included with the evaporator was a quartz crystal monitor that was never used due to fluid dynamic considerations mentioned above. Four different configurations influenced by previous depositions were used over the course of the experiment. It is important to note that mirror substrates produced good results independent of setup.

Explanations of each configuration are written below with general descriptions and observations of deposition results. Individual results are published in the appendix.



(a) Second setup: Simple Water cooling

(b) Third setup: Improved Cooling

Figure 2: Water cooling setups of the evaporator

### 2.3.1 First setup, stock

The stock system was not cooled. It was comprised of a shelf that supported a substrate holder, three pairs of copper leads, and a shield covering the system. Two mirrors were placed in such a way as to observe the sources melt and evaporate. A hole had been cut into the shield for the user to look into the mirror. Source-to-substrate distance was approximately 8.3in. The boat sat at the bottom of the evaporator connected by copper leads. Films produced were found to be blistering hot soon after each evaporation and required a cool-down period before being handled. Metals tested in this setup included indium and copper.

### 2.3.2 Second setup, elevated boat

After producing copper and indium films it was determined that improvements were necessary. Moving the boat up and the substrate holder down reduced the boat to source distance. A copper bridge made of copper blocks attached to the substrate holder and was held up by the quartz crystal monitor. Reducing the distance to 5.3 in without changing the mean free path lowered the required deposition time.

Not many samples were deposited using this setup. Copper had been deposited in this system with decent success before the evaporator was modified further. Without water cooling it was assumed no other useful deposits could be made so water cooling was quickly added.

### 2.3.3 Third setup

Water cooling was added as shown in Figure 2a by exploiting the thermal copper bridge holding the substrate holder. Films were cooled by treating the bridge as a thermal tube and running water through the quartz crystal monitor. There were two thermal junctions: a copper block screwed onto the quartz-crystal monitor followed by two copper blocks, attached to the first, suspending the substrate holder. Pipes feeding the water to the crystal monitor were 1/4" outer diameter fed by cooled industrial water from the building. Although the crystal monitor itself remained cool, the amount of heat transferred to the water was limited.

Unfortunately this setup was not a permanent solution as the deposition time was still limited by the amount of heat absorbed in the system. A housing was made to include a wider variety of substrates and substrate distances. The substrate holder held up a housing, much like a skirt, made of copper foil. There is an opening in the skirt for the mirror on the right of Figure 2a to see the boat. Dimensions of the skirt are 5" diameter, 4 1/2" tall, and 3 1/4" tall at the opening for the mirror.

Deposition time improved in this setup but was still limited to about 20 minutes before some films became discolored and less black. Longer deposition times usually resulted in poor results but also depended on the type of metal deposited.

Many different setups and metals were tested in this configuration. Aluminum foil as well as substrates on the holder and mirror were observed to have different amounts of blackness depending on the metal, deposition time, and distance. Aluminum foil placed on the skirt often had good to great results. Details are in Appendix C.

### 2.3.4 Fourth setup

Final design considerations required that the substrate be moved even closer to the boat source and provide improved water cooling integration by using soldered contacts between tubing and substrate holder. Removing the quartz-crystal monitor resolved space issues and new pipes were installed. The last setup has a source to substrate distance of 5cm and 1/4" water pipes soldered to a large copper plate of dimensions: 6.02in x 5.42in x 0.125in. Chilled water circulated by means of a reservoir entered and exited the chamber through about 1.5 feet of tubing. Pipes were soldered on to the copper plate using bricks, a hot plate, lots of flux, and solder. Swagelok connections ensured leak-free connection during vacuum operation. Substrates were clamped on by thin copper plates to ensure good thermal contact.

Copper foil is the most commonly used substrate in this configuration. Two thin copper bars hold the foil up the breadth of the deposition to happen between them. Metal black is deposited primarily between the clamps but also on a hanging edge of the foil a few inches away.

Results in the configuration were unusual in that films produced were initially darker than any others films produced over the lifetime of the project. Consequences of this new setup was a transparency of some of the films when left alone over an order of a couple of days. Immediately after opening a high reflectance portion of the films is visible to the eye at the position between the two clamps. Copper and tin samples were made and found to have both turned transparent in the region of the film that had higher perceived reflectance. Transparency is probably due to oxidation of the films due to a finer nanostructure as a result of a lower source to substrate distance. Finer structure allows for a higher surface area of metal black to face the air and oxidize. Tin left in Argon over a long period of time, about 11 days, was found to have a high degree of reflectivity between the clamps but very little on the free-hanging edge. The sample did not turn transparent, unlike the previous tin film.

### 2.3.5 Zeroth setup: no substrate holder or cooling

Without cooling or a holder metal black films were possible to create under two conditions: overhanging copper foil and using a mirror substrate. All mirror substrates did not have any water cooling but retained a large amount of blackness over the course of many depositions. On some occasions mirror substrates were the only substrate to receive black results at all. An attempt at making better samples was proven successful when a large piece of copper foil was placed above the boat in a manner such that it resembled a circle with the center at the boat source and an average radius of 4.5 inches. These films proved to be the very best out of all samples. In contrast to the fourth setup these films retained their blackness over multiple weeks. Similarly mirror substrates also retained their blackness and are examples of some of the darkest films.

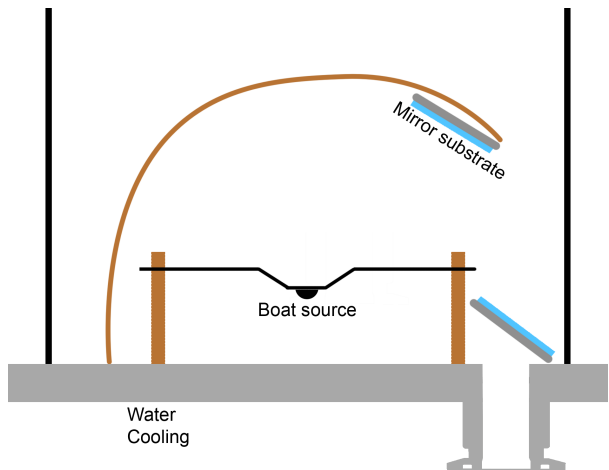


Figure 3: Zeroth setup: Hanging Copper Foil

## 2.4 Observations and Resulting Films

Visual appearance of the films is one of the main indicators of an underlying nanostructure. Finer-scale structure generally corresponds to lower reflectivity in the metal black films synthesized under these conditions. For this reason we use the films' appearance as an indicator of the success of a deposition. Observations of the black substance deposited around the machine hold possible clues to the physics of deposited metal black. Setup four, for example, often deposited thick metal black on the tubing above the plate, implying that the coldest object in the evaporator is often the best substrate even when it is not line-of-sight to a source.

Usually over long deposition times discoloration occurs on all line-of-sight substrates. Films created on the mirror substrate are found to have characteristics similar to high vacuum deposits when left alone for too long. Similar discoloration happens when a high powered LED shines on the films on a focused spot. For silver and copper the spot is a light grey color. One guess as to why the discoloration is grey and not the color of the metal is a gradual increase in reflectivity as the nanostructure is reshaped.

Pure white depositions occurred for magnesium and silver deposition on free hanging copper foil substrates. For silver the deposition was done at uncharacteristically high amperage (191 amps at max over 2 minutes). In contrast magnesium required a very low current in order to melt and produce a thick film. These unusual results offers insight on the role deposition rate has on the blackness of films: extremely large deposition rates tend to produce lighter films distinct from the normal coloration of the metals in bulk.

Aging of the films that was observed in the fourth setup is speculated to come from two possible sources. Possible oxidation of the films closer to the source may occur at a rapid rate if a finer structure exists. Another speculation is the rapid heating of the film surface during deposition. Heating with little thermal coupling may lead to a change in structure of the films.

## **Elemental Techniques**

A major results of this thesis is the determination of good deposition parameters for nine different metals (for details on depositions see Appendix C). Techniques to obtain the visually blackest films for each metal as well as other observations are described below.

### **2.4.1 Copper**

Copper can be evaporated with best results using currents around 180 Amps and pressures around 5 Torr. Depositions are usually very quick and a good copper sample can be produced in less than 10 minutes. Boat types used to create good films include molybdenum and molybdenum coated with aluminum oxide. Many depositions using the aluminum oxide coating causes previously melted copper to stick to the coating and remove a portion of it when handled. Although copper will stick to most substrates it requires a wetting layer on glass to adhere well and adheres the best to copper. As a result the best results are on cooled copper foil. Most mirror substrates produced great results on black copper.

Differences between cooled and uncooled copper foil substrates were observed. Uncooled copper foil produced uniform results under quick depositions. Cooled copper foil using the large cooling plate produced extremely black samples initially. Over time the body of the sample became transparent and dull.

### **2.4.2 Silver**

Silver is deposited with good results at around 180 amps and 5 Torr. Results and parameters are similar to copper. White silver can be produced if deposited over long periods of time.



Black silver has been produced successfully and reliably on mirror substrates and overhanging copper foil.

### **2.4.3 Aluminum**

Aluminum was one of the hardest samples to evaporate and deposit. Good samples were hard to come by and the process tested the limits of the evaporator. Most depositions involved the boat breaking and in some occasions automatic shut-off by the evaporator. Aluminum was the metal that required the highest energy to evaporate at over 200 amps. At this current if left on long enough the evaporator is likely to shut itself off by flipping the SCR relay.

First successful melting of aluminum was over the course of a short period of time using a large boat and large heavy samples of aluminum (see Appendix C.6). The aluminum came in large pellets on the order of a few tens of grams which resulted in poor thermal conductivity and large heat capacity. Precluding the first successful melting of aluminum was a failure: a first pellet placed on the left side of the boat did not melt and instead developed a layer of matte grey film around it. Current was raised to 230 amps over the course of an hour until the SCR flipped off. After the failed evaporation another pellet was placed next to the first and the current was raised to 220 amps in 15 minutes. The second pellet melted first and finally the original pellet, with its grey film, also melted. Despite the success of melting aluminum the evaporation was a failure and only a grey film was produced around the entire evaporator.

A later deposition of aluminum produced a dark brown coloration. Using a quicker ascent to higher currents resulted in successful development of films. Although not ideal, the process was attempted again. One good deposition, with details in Appendix C.8, was obtained and saved. This used a sawed off piece of aluminum and a smaller boat covered with alumina oxide. This deposition was very black; one of the darkest samples ever created. Unfortunately although multiple attempts were made no other black sample of aluminum was synthesized afterwards. Later attempts used similar methods to the black deposition. Smaller pieces and boats were used but only produced successive grey results.

### **2.4.4 Iron**

Iron produced good results. Iron only had black samples that were easily produced. Over time the iron films turned a brownish color similar to rust, an event expected due to the high surface area of the films. Best results were produced on an overhanging copper film. Second best results came from the mirror substrate although iron does not adhere well to glass.

Black films thin out towards a dull brown on most films. The light brown is probably

due to the rusting of iron. Most obvious examples of brown are samples of iron left in air for multiple days.

#### **2.4.5 Chromium**

Chromium films were produced using a chromium-plated tungsten rod. Results were poor and full of chromium oxide due to a sudden accidental venting of air. A ball valve suddenly opening caused air to rush into the evaporator and raise the pressure. Resulting effects include sudden smoking and an increase in intensity of light from the tungsten filament. Smoke was seen moving across the chamber and producing a growth of films on almost every surface. After re-venting and letting the system cool down the bell jar was opened and cleaned. Convection currents that were seen are assumed to be the cause of the massive production of films adhering to almost every surface in the evaporator. Substrates taken on foil, glass, and the substrate mirror were grey with green. Chromium oxide is known to be green and is assumed to be the primary compound in the films. No other chromium depositions were attempted due to the foreseen lack of useful applications.

#### **2.4.6 Gold**

Gold was obtained in very limited quantities, enough for a couple of evaporations, for the experiment. One deposition was made with a large amount of substrates with varying distances. Unlike other elements gold is limited and therefore it is difficult to find ideal deposition parameters for the metal. Many samples were produced of various distances and quality. Substrates closer to the boat produced the best black deposition especially on mica and copper. Gold did not adhere well to glass. Evaporation was seen at currents of about 200 amps and was kept on until a relay flipped and the SCR turns off. Total time for rapid deposition was about 5 minutes.

#### **2.4.7 Indium**

Indium was extensively deposited and explored due to the possibility of novel superconducting properties that may appear with changes in structure. Indium deposits at low amperage, around 140 amps. Fastest depositions happen at 5 Torr. Best substrates for the darkest Indium are copper foil but glass also works well. True black Indium has never been achieved although numerous attempts were made. One of the problems may be due to the difficulty of seeing indium melt after the boat source becomes incandescent enough to see the sample. Since the rate of deposition is evaluated by looking into the evaporator's bell jar only ultra-fast depositions can be seen in Indium evaporations.

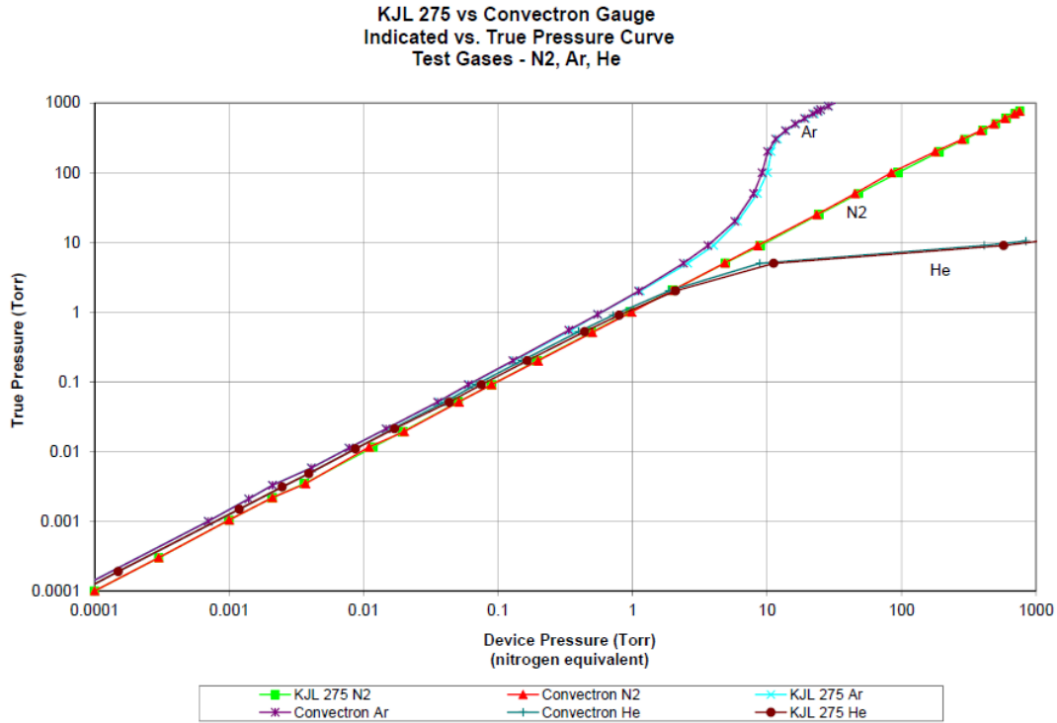


Figure 4: True vs Measured pressure in different gases for 275 type convector gauge[1]

### 2.4.8 Magnesium

Magnesium was evaporated at 140 amps. Vapor pressure of magnesium is much higher than indium at a given temperature. Resulting deposition times are therefore much shorter (due to higher deposition rates) for the same amperage. Resulting films on a copper foil substrate were matte white. After SEMing silver white it was found that the sample is actually melted. Assuming the same thing happens to magnesium then the deposition needs to run at a lower amperage to prevent a rate so high that the magnesium melts and wets its substrate.

## 2.5 Vacuum sensors and controller

A Terranova 907 vacuum sensor controller connected to a Diaphragm vacuum sensor is used. The Terranova is a digital gauge that has automatic adjusting for Argon environments. Dual vacuum gauges allow for a larger range of accurate vacuum pressure output from 1 mTorr to room pressure. The convection gauge stops working well in Argon at about 5 Torr, as seen in the figure below, so it was decided to include the diaphragm gauge as well. Diaphragm gauges are gas independent pressure sensors and as a result provide true pressures if calibrated correctly. Convector gauges are gas dependent as they rely on heat transfer from the surrounding gas to obtain pressure measurements.

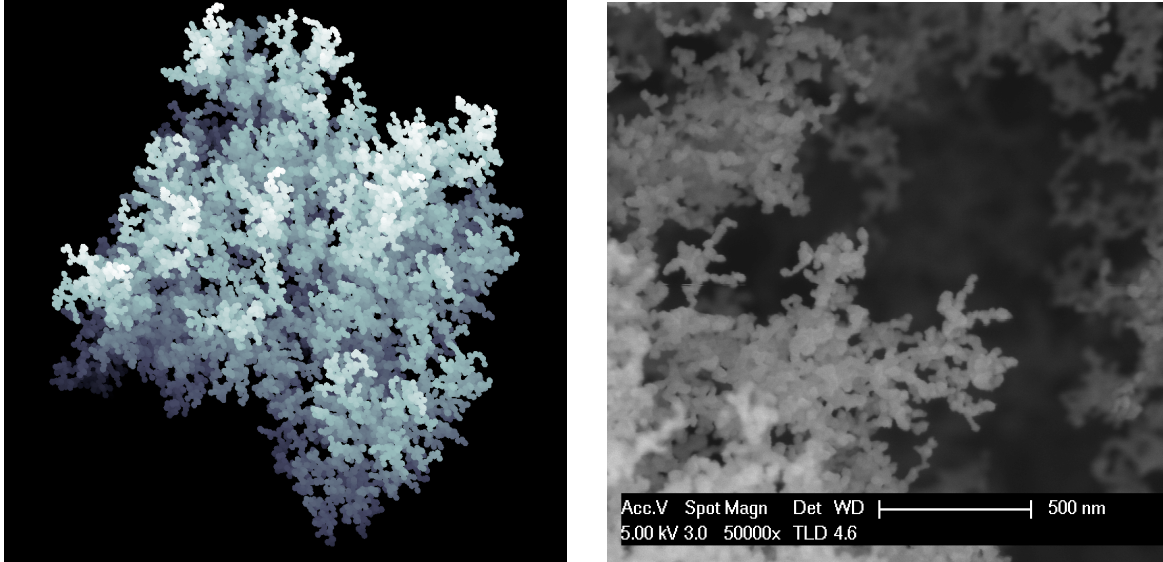


Figure 5: Comparison between simulated and metal black DLA

### 3 Morphology

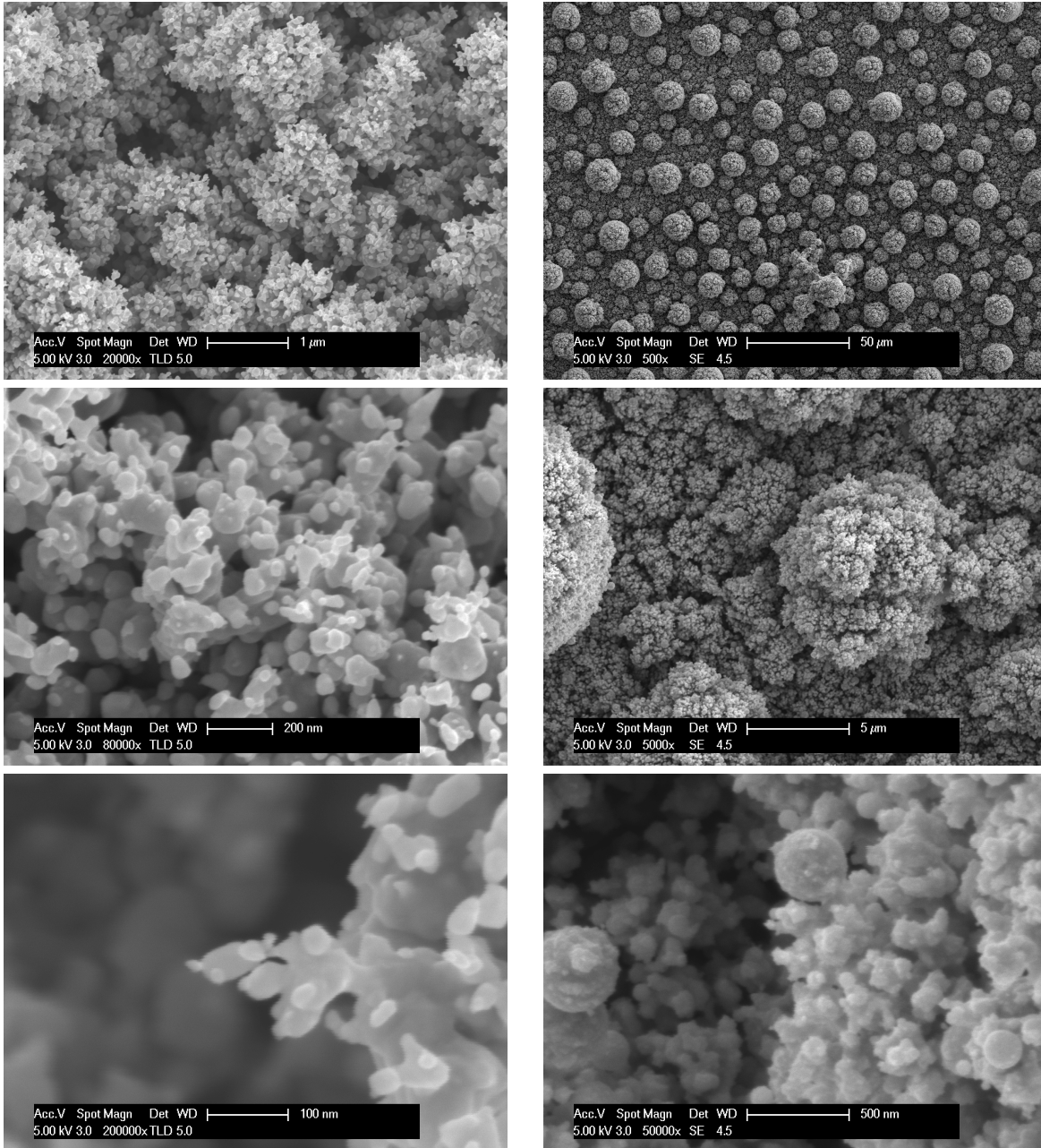
Under visual inspection the films range from a “velvety” black to a dull grey to white in extreme conditions. The best films look as if a fine carpet of dust has settled on the substrate. Indeed the films can be scraped off and put into a dark pile of fine velvet. SEM images were taken of the films and a summary of the results is reproduced below.

#### 3.1 SEM results

Metal black films appear porous and stochastically nano-structured under SEM. SEM imaging of Indium, Copper, Aluminum, and Silver of various age, deposition parameters, and conditions were taken. Correlation between films and varying degrees of darkness is somewhat apparent without appreciable results. The darkest films tend towards being more porous and have a finer structure than films that are less dark.

The SEM results shown in Figure 6 are the result of depositing silver and indium separately onto a copper foil substrate. Results show that the structure of silver is on a much finer scale than indium, a common feature of black films apparent in Figure 8 as well.

Other features common on most SEM’d images are larger “balls” of material on the micron scale apparent in most black samples. Other, less black, samples are amorphous such as the gray silver in Figure 8 and 9. Grey silver and thin parts of aluminum black appear amorphous in structure especially where compared side-by-side to other SEM images.



(a) SEM Images of Silver. Deposited 3 inches from source at 7 Torr for an hour and 20 minutes. 1: micron scale, 2: 200nm scale, 3: 100nm scale.

(b) SEM Images of Indium. Deposited 3 inches from source at 5 Torr for 43 minutes. 1: 50 micron scale, 2: 5 micron scale, 3: 500nm scale

Figure 6: SEM images of Silver and Indium at different scales

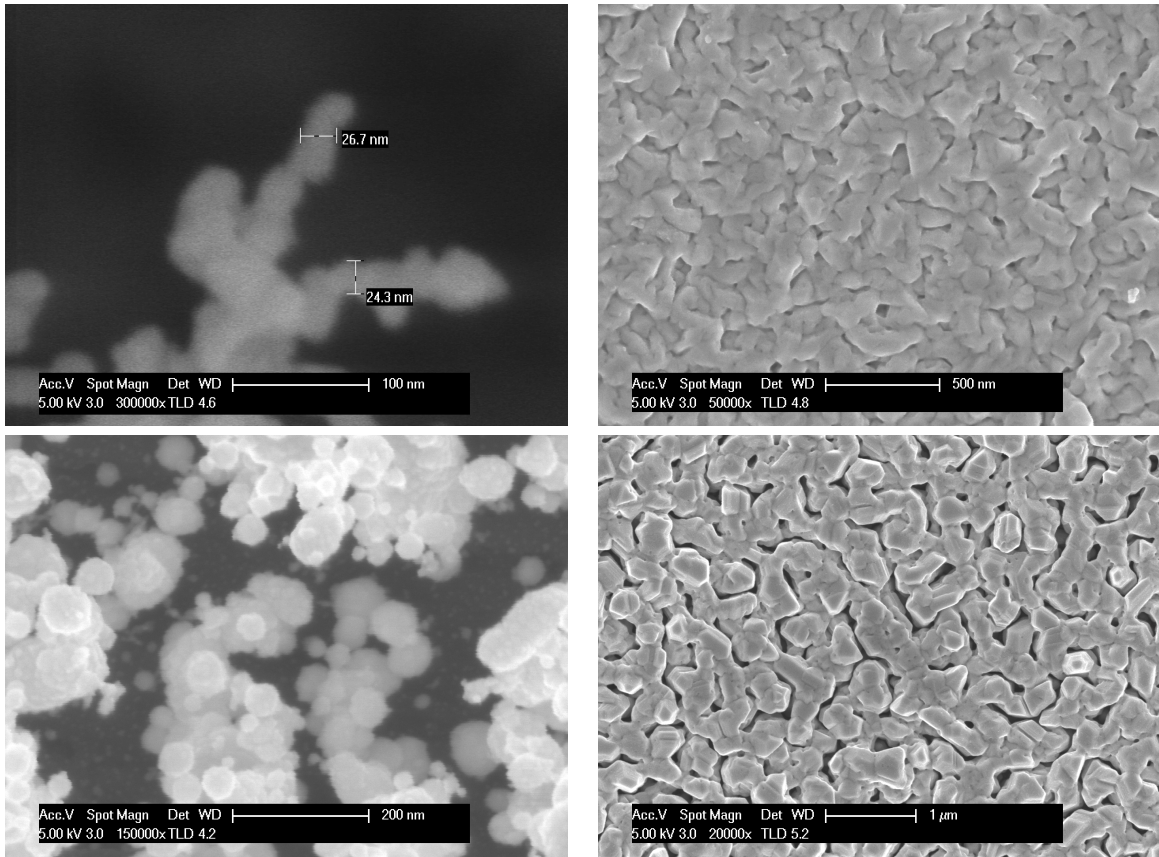


Figure 7: Some interesting SEM images  
 Top left: copper with 30nm wide tendrils. Top right: high vacuum deposited copper.  
 Bottom left: indium black sample on glass.  
 Bottom right: white silver evaporated for a long time (1 hour)

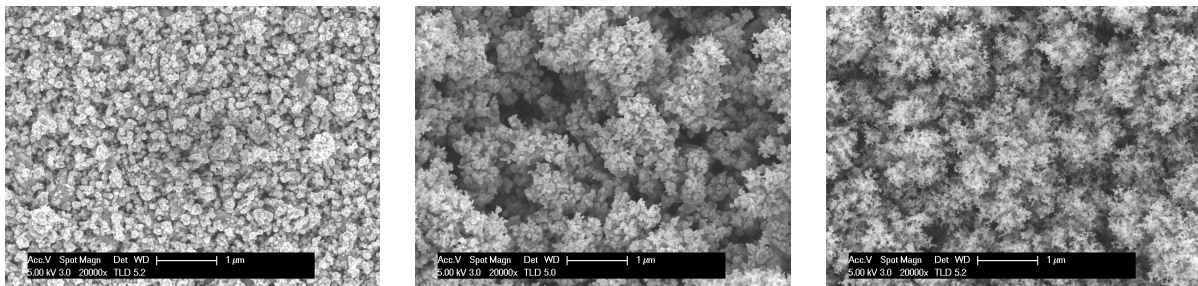
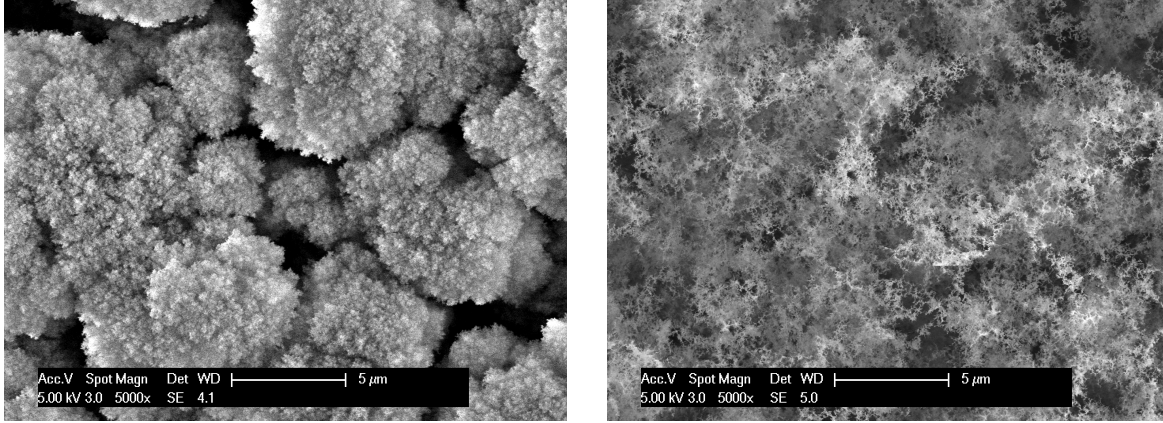


Figure 8: Gray Silver, Black silver, and Black copper side-by-side at 20000x magnification





(a) SEM Images of “black” Al.

(b) SEM Images of “blue” Al.

Figure 9: Nanostructured Aluminum

### 3.2 Assumptions based on SEM results

In metal black it was theorized (before SEM pictures were taken) that the particles needed to have a [semi]-random encounter with the substrate to simulate a random walk[5]. Events during deposition were also surmised to behave such that if the metal collided with a cold substrate a diffusion limited aggregation growth would occur a few atoms at a time. This theory was soon struck down based on the results of SEM images taken. From the simulation in Figure 5 we can see that there is high correlation between metal-blacks and DLA in three dimensional space. Such features cannot come from individual atoms so the formation of the structure is assumed to takes place in the gaseous phase before contact with the substrate. The resulting aggregates fall as “metal snow” onto the substrate where DLA structures would strike the substrate and stick under the same mechanism that resulted in its formation. Large spheres of atoms might be explained by the aggregation of DLA structures to form even larger structures.

## 4 Optical Properties

The optical properties of metal blacks are dominated by the low reflectivity of the films. During synthesis reflectivity of films was judged using visual inspection. Reflectivity measurements were later done on a few different films in order to obtain quantitative measurements. The reflectometer uses an integrating sphere to measure the light reflected off a sample contrasted with a reference sample as given by

$$R(\lambda) = \frac{\text{Reflected power at } \lambda}{\text{Total power sent at } \lambda}$$

## 4.1 Reflectometry

MRL TEMPO facilities were utilized to find the reflectance of the films. A Shimadzu V3600 UV-Vis-NIR reflectometer took over a thousand individual measurements in the wavelength range of 440nm to 2600nm. Reference (or baseline) samples of  $\text{BaSO}_4$  were used and compared to another powder sample of  $\text{BaSO}_4$ . Comparisons were then normalized it to 1 (or 100%). After that a reflectivity measurement of a sample is made by comparing the reflected light to the  $\text{BaSO}_4$  sample.

The baseline sample used has an average reflectance of 100.04% and a variance of 0.0028. The discrepancy from the normalized 100% is due to a combination of noise from the machine itself and changes in the reflectance of  $\text{BaSO}_4$ .  $\text{BaSO}_4$  reflectivity at wavelengths less than 400nm is smaller than 100%<sup>[9][7]</sup>. Noise enters the system most noticeably when the signal to noise ratio drops. Lack of light, reflected or otherwise, reduced the signal and prevents a good baseline.  $\text{BaSO}_4$  is not a perfect reflector in all wavelengths and therefore will have a greater amount of noise at the high and low bounds of the wavelength measured in the reflectometer.

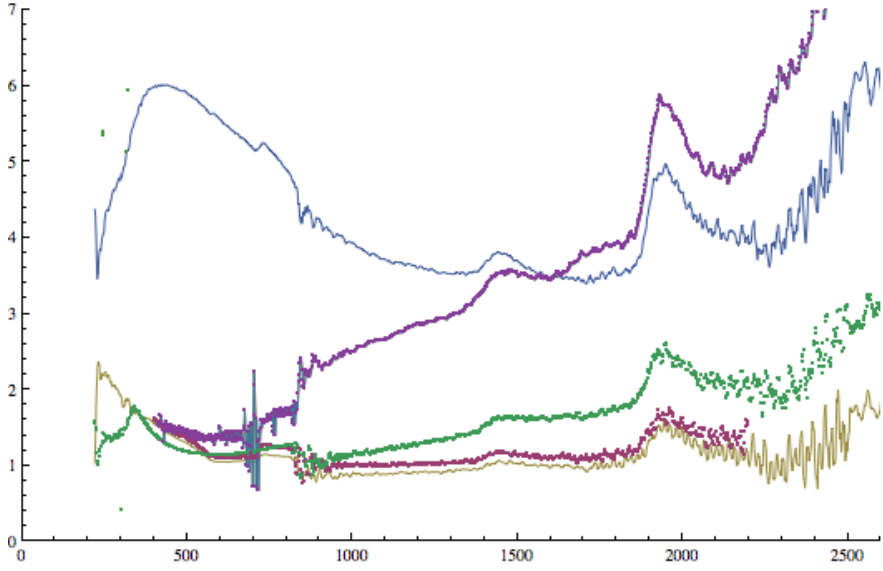
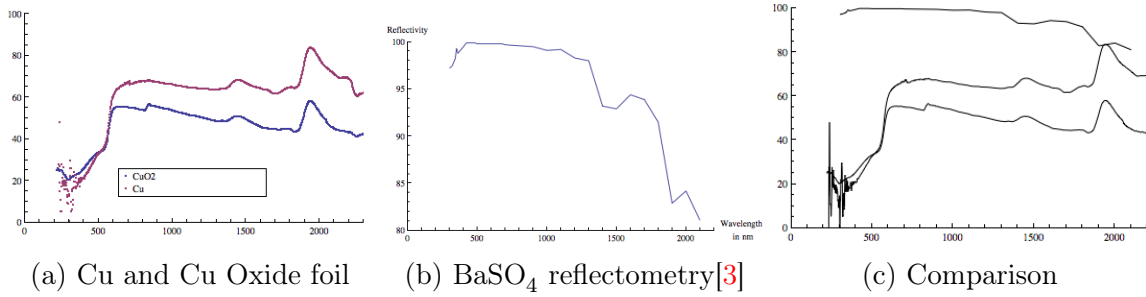
The reflectometry results appear with strange characteristic bumps independent of substrate and metal used (see Figure 10c). These curious results are due to the non-ideal reflectance of  $\text{BaSO}_4$ . In Figure 10c we see that the Copper foil and Copper Oxide foil (slightly darker foil that has been left in open for a period of time) have the characteristic bumps seen in all samples (Figure 10d)

Two of the best (visually black) samples measured were copper and silver, both deposited on copper foil. Both samples have visual characteristics indistinct to the human eye. Mean reflectance between 220nm and 2600nm of silver and copper samples are 1.66% and 3.84% respectively. Due to the discrepancy in the data received from the V3600 (due to the change in reflectance of  $\text{BaSO}_4$  at wavelengths below 400nm and above 2000nm) data lower than 400nm and higher than 1700nm is thrown away and the mean is recalculated. Between 400nm and 1700nm Silver and Copper have a reflectance of 1.31% and 2.69% respectively.

## 5 Photoacoustic Properties

The photoacoustic effect, a phenomenon common to almost all materials, was discovered by Alexander Graham Bell <sup>[2]</sup>. Photoacoustic phenomenon can be described as the “ringing” of material when exposed to rapidly switching light. Recently popularization of the photoacoustic effect resulted from the discovery of applications across multiple disciplines<sup>[10]</sup>. Although many materials have an audible photoacoustic response metal black films were found to be





(d) Many different sample. The lower results are all black.

Figure 10: Reflectometry results

Three graphs comparing Copper peaks with BaSO<sub>4</sub> peaks and one with many different samples. The last graph in order of samples that end on the right from top to bottom: copper on aluminum foil, indium on copper foil, silver on copper foil, old copper on aluminum foil, copper on glass

noticeably louder. Rediscovery of the photoacoustic effect in the Weld lab prompted interest in characterizing the effect. Shining a bright pulsing LED flashlight onto the films caused a large response audible within a few inches. To obtain better qualitative results an apparatus was built to measure the effect.

## 5.1 Theory

A rigorous theory [11], dubbed the Rosencwaig-Gersho Theory, has been published in order to try and explain the phenomenon. The paper agrees with experiment up to high frequencies[10]. The photoacoustic effect was initially thought by the Weld lab to be due to the films' thermal expansion. The R-G theory asserts that this theory is incorrect and the photoacoustic signal comes from the heating of the gas in contact with the material.

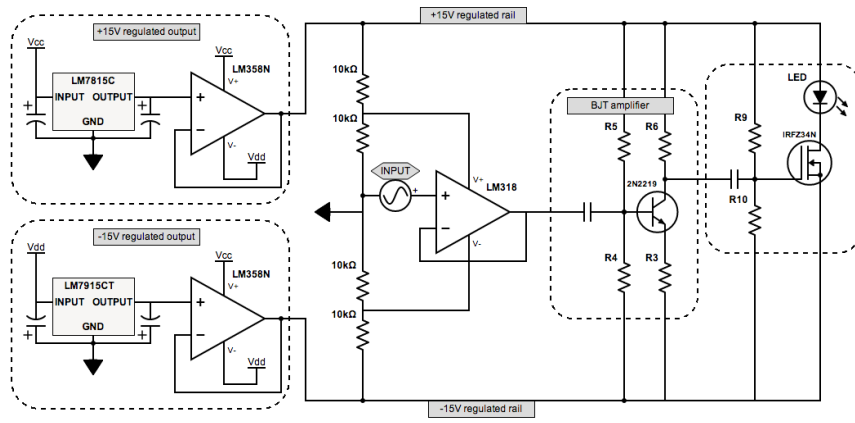
Transparency is said to also play a role in producing louder photoacoustic results. The reasoning is that light heats up more gas within the layers of the material in question. Resulting heating of the gas produces a larger pressure wave and therefore a louder result.

## 5.2 Experimental Setup

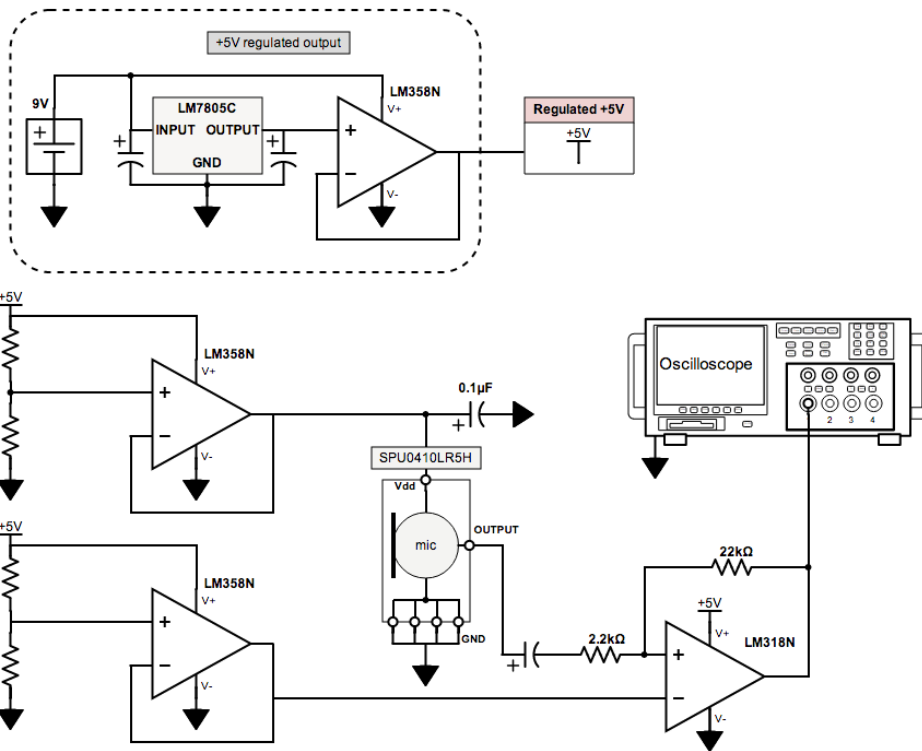
The goals of this part of the experiment are to find the photoacoustic range and the frequency vs amplitude response of metal black films. Higher frequencies are inaudible to human ears and requires microphones capable of receiving ultrasonic frequencies.

Three setups were used for this experiment with the purpose of finding the frequency versus amplitude response of the films. An acoustically dampened environment was built to house the experiment. Bright light pulses were directed at a nanostructured film in a small but dense wooden container filled with foam. The circuit for the light (see Figure 11a) is capable of driving an LED light up to 30V at frequencies exceeding 130kHz. Inputs accepted are square waves with arbitrary duty cycles. For best response, the LED should be greater than 200 lumens. The primary LED used is 1000 lumens.

A high-powered LED mounted on a aluminum heat sink was used to stimulate the most powerful photoacoustic effect possible. These LEDs are round disks half an inch in diameter and films are about 2" by 2", the same size as the heat sink. Films are set in such a way so that the light from the high-powered LED is at normal incidence. Placed a distance of about 3/4" the film is exposed to over 60% of the total flux of light from the LED. Dark films left in the apparatus longer than a few minutes start significantly heating up due to their high absorbance. Over periods of time on the order of 10 minutes films on copper substrates become scaldingly hot and films on glass visually change into a discolored state. Discoloration is especially prevalent on glass substrates. Thermal conductivity of glass, as stated earlier,



(a) Flashing light circuit



(b) Microphone circuit

Figure 11: Circuits used in the photoacoustic experiment

is much lower than copper (the thermal conductivity of copper is 400 times that of glass) so films on glass likely heat up quickly with minimal thermal flux into the substrate. Some films now have a obvious circular discoloration on the surface when overexposed to bright LED's or camera flashes.

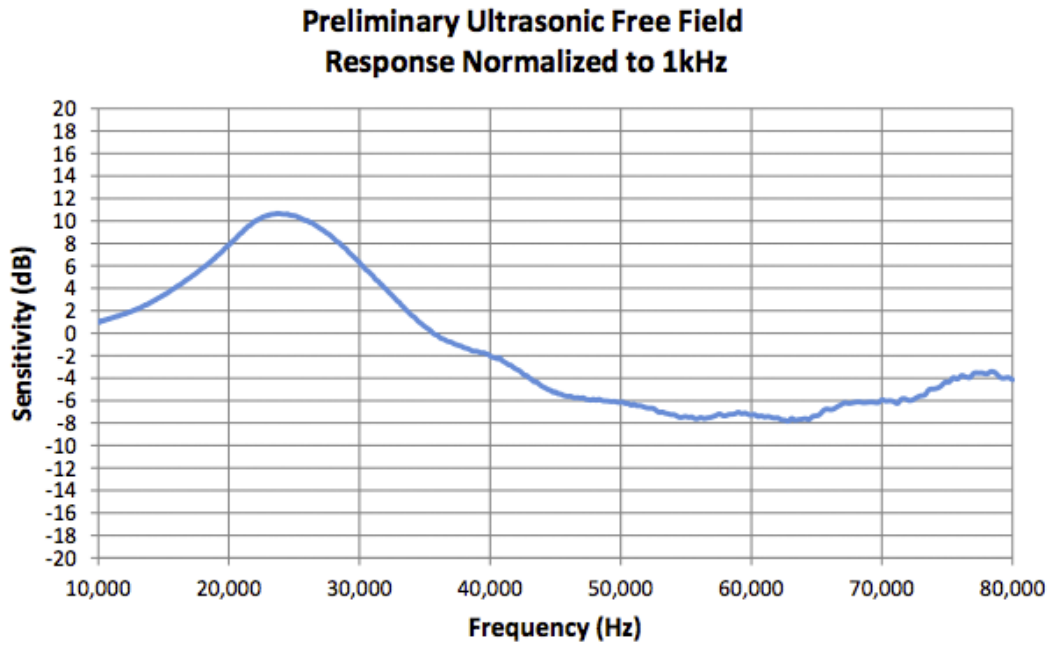
In order to verify pulsing of the LED at higher frequencies a Thorlabs photo-diode (model PDA100A Si Amplified Detector) was placed in the path of some reflected light from the LED. Phase effects due to reflection were expected not to exceed the 150ns response time of the photodiode and therefore ignored. There was no noticeable phase gap between the input waveform and the output light intensity as long as a square wave was used.

The first system used a 20kHz microphone (called the cheap mic) to obtain data. Little qualitative data was recorded using the cheap mic but the process was recorded and reproduced using a better 100kHz MEMs microphone (called the MEMs mic). Placing the cheap mic a short distance from the film and watching the output on an oscilloscope produced interesting results that resulted in the following conclusions about the setup when driven from 5kHz to 15kHz. Firstly, phase difference of the light and the generated acoustic wave differed by a time defined by the distance to the microphone divided by the speed of sound. Secondly there were two observable echoes: one from the substrate to the LED mount and another from the microphone to the substrate. Finally, interference between echoes occurred depending on the frequency of the light modulation.

Echoes were verified by moving the cheap mic closer and farther from the source substrate and measuring an interference phase change. Placing the mic behind the source substrate removed one set of echoes but left another set of echoes assumed to be between the heat sink and the substrate.

A SPU0410LR5H MEMs microphone with a frequency response past 100kHz was used for further experiments. Frequency response for the MEMs mic was plotted by a third party and replotted using the program "Graphclick" by Arizona Software. Using the given data it is possible to extrapolate the sensitivity and find the actual amplitude of sound at any given frequency. In Figure 12 the second graph features a conversion from dB to volts where a reference voltage of 1V was used. Finding the actual amplitude from measurement data is done most easily by dividing the amplitude displayed on the oscilloscope by the sensitivity.

Silver deposited on copper foil was used to obtain preliminary results for frequency versus amplitude using the high-powered LED. Figure 13 shows a plot of frequency versus amplitude using raw data obtained by simply changing the frequency. As the figure shows, there are beats being recorded by the oscilloscope in frequency space that correspond to constructive and destructive interference. Graphs of sensitivity versus frequency of the MEMs microphone is displayed in Figure 12. Since the frequency versus amplitude is essentially oscillating



From page 3 of [http://www.knowles.com/search/prods\\_pdf/SPU0410LR5H.pdf](http://www.knowles.com/search/prods_pdf/SPU0410LR5H.pdf)

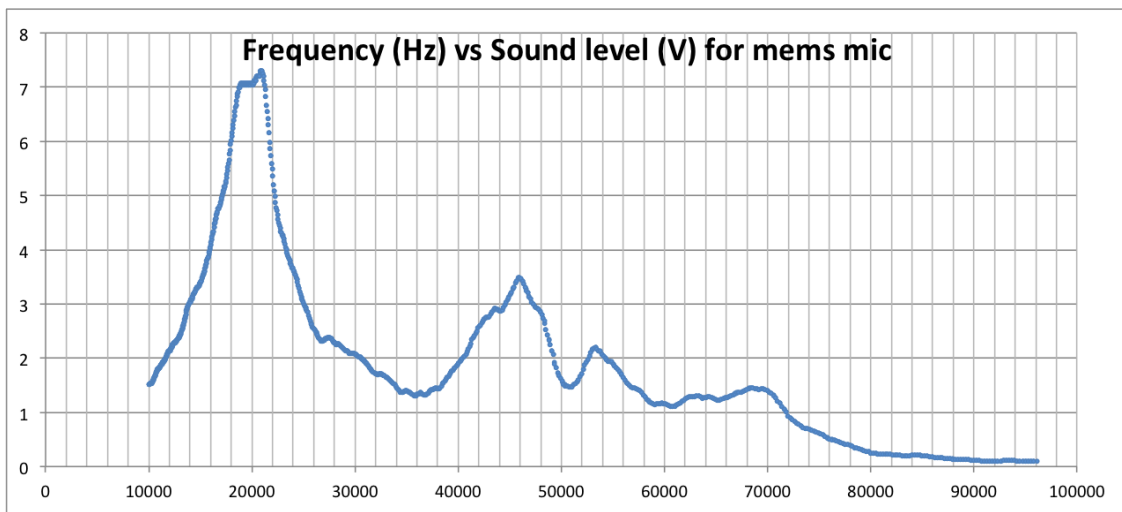


Figure 12: SPU0410LR5H MEMs microphone response with respect to frequency

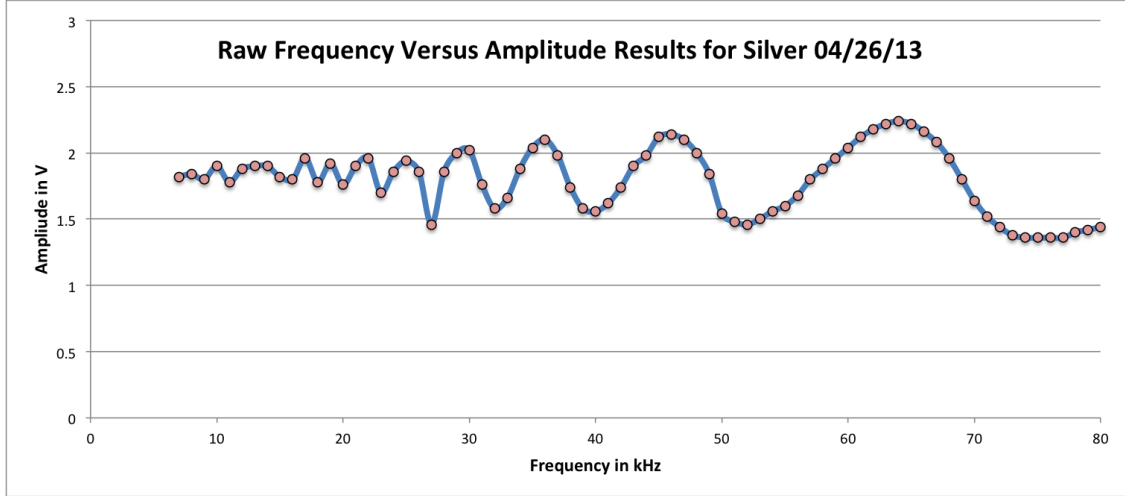


Figure 13: Unusable frequency versus amplitude measurements dominated by electrical coupling

around 1.7 V it fails to reflect the sensitivity of the microphone. Thus we expect this measurement to be determined by electrical coupling.

A consequence of using a high powered LED was the large amount of electrical interference that comes from switching large currents. Verification of interference was made by oscillating the distance between the LED circuit and the coaxial cable feeding the LED. Close proximity to the current carrying wires of the LED circuit induces response on the oscilloscope in phase with the electrical signal feeding the LED circuit. To combat the effect of interference lasers owned by the Weld Lab were used in the experiment in an attempt to circumvent noise from the LED circuit. The laser system used a 671nm red laser on the order of 200mW. An AOM was used to amplitude-modulate the laser and a convex lens was used to increase the beam size.

### 5.3 Results and correlation to theory

As stated above there were two microphones used in the experiment testing the photoacoustic effect on metal black films. Higher frequency measurements corresponds to higher resolution of data so only the MEMs mic data is discussed.

Screenshots of the MEM's response with the laser setup is found in Appendix D. Data displayed shows different waveforms between 10kHz and 20kHz and the MEMs response. Resulting waves are seen to constructively and destructively interfere in between two larger peaks. As stated earlier it was found that electrical coupling played a significant role in the results shown on the oscilloscope. Resulting waveforms are therefore probably interfering with the actual data received by the microphone. Extracting data is possible under these

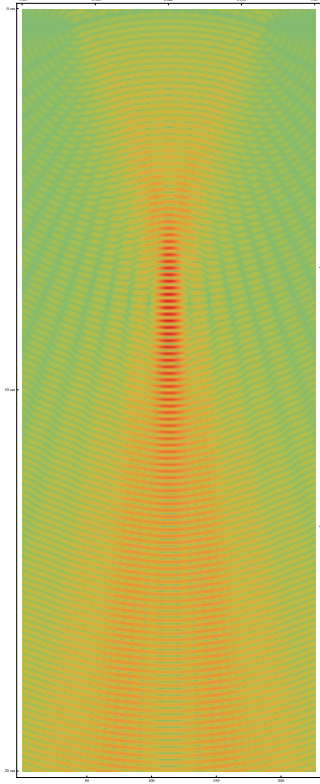


Figure 14: Focused photoacoustic intensity using planoconcave lens

conditions but it was decided that a more worthwhile expenditure of time would be to create an experiment lacking electrical noise.

The photoacoustic effect can be reproduced on most surfaces. Much stronger response is on films that are the blackest followed by grey films. Films that are white in color produce no clear audible signal but require experimental verification using microphones.

## 5.4 Acoustic Phased Array

A idea that stemmed from the photoacoustic effect was the creation of simple acoustic phased arrays by depositing metal black on a plano-concave lens. By shining a pulsing light on the flat side of the lens an acoustic wave is generated on the concave side of the lens. Interference produces a focused spot of high acoustic intensity. A simulation of the resulting wave for a 100kHz incident pulsing light is appears in Figure 14. The algorithm used to determine the intensity simply sums over all points on the lens relative to a point on the graph. High intensity waves are in red and low intensity waves are green. Possible applications include easy and cheap production of high-intensity ultrasonic sources for imaging.

## 6 Conclusion

Metal black films were produced using novel evaporation techniques. In contrast to high vacuum thermal evaporation, low vacuum evaporation is a non-standard process that dirties the evaporator. Synthesis of nanostructured films does not require expensive computerized thermal evaporators to keep constant pressure and temperature. Films are forgiving in sudden change in pressure on the order of hundreds of mTorr and only require short deposition times in order to be successfully deposited as metal black. The “forgiving” nature of DLA can also be seen from the apparent similarities between our parameter-free simulations of aggregates and the actual morphology of the films (see Figure 5). Resulting growth of metal black films is therefore cheap and easy consequentially producing incentive to explore the films.

Deposition parameters were determined for nine different metals. Each element was observed to produce different results from the configurations described and as a result have slightly different optical properties. Deposition quality also played a role in the resulting blackness. It was determined that deposition distance has a much greater effect on blackness than any other parameter such as water cooling.

Exploratory measurements of the optical, photoacoustic, and physical properties were taken and discussed. SEM results show that the darkest metal blacks are not amorphous and resemble a diffusion limited aggregate (DLA) in three dimensional space. Metal blacks are seen to have large structures on the micrometer scale that resemble a quilt on top of the finer DLA structure. Physical characteristics were observed to change with time in some films. Lastly, photoacoustic measurements indicate that the films are capable of responding to incident light flashing at frequencies past 50 kHz which indicates possible applications in focused high frequency acoustic generation.

### 6.1 Avenues of further research

Many different opportunities for exploration of metal black films are available. Synthesis of the films involved a small subset of evaporation techniques available despite lack of automation and precision. Further modification of the evaporator and procedural improvements can continue indefinitely to provide more consistent results.

Photoacoustic measurements without interference from electrical noise are necessary to successfully measure the frequency versus amplitude response of the films. Recreating the photoacoustic circuit to reject noise is necessary to receive usable data. Determining the ability for photoacoustic films to produce ultrasonic waves provides the framework necessary to build and explore acoustic-phased arrays.



Developing code to analyze SEM measurements to determine the fractal dimension is the next step in characterizing the scaling of nanostructured films. By using algorithms that take depth and shadows into account it is possible to compute the fractal dimension will help to further understand the process in which these films form. Further DLA simulation code that takes sticking probabilities and mean free path into account also holds potential enlightenment on the formation of the films. The closer the simulated structure is to real films the better we can understand the formation of the films.

X-ray Diffraction measurements (XRD) provide information on the atomic structure of a given sample. Using XRD on films that have aged and comparing them to those that have not may provide insight on the mechanism that causes the films to decay, turn transparent, or change color.

# Appendices

## A Mathematica Code

### A.1 Photoacoustic Simulation

Listing 1: Acoustic Phased Array simulation

---

```
1  (*constants: R is radius of curvature for lens, d is diameter,
2  c is speed of sound, w is width of plane*)
3  R = 0.0772; d = 2*0.0254; c = 340; w = 3*0.0254;
4  findIntensity = Function{freq},
5  period = 1/freq;
6  lambda = c/freq;
7  lensepsilon = Min[lambda/5, 0.001];
8  planer = Range[0, w/2, lensepsilon];
9  planez = Range[0, 0.20, lensepsilon];
10 intensity = Table[
11   Total[ Parallelize [Table[
12     Cos[(-2*Pi*freq*tt) + (
13       (2 Pi/lambda)*Sqrt[((RR - planer[[r]])^2 +
14         ((planez[[z]] - (R - Sqrt[(R^2) - (RR^2)]))^2)]),
15       {RR, -d/2, d/2, lensepsilon}, {tt, 0, period, period/30}], 2]^2
16   , {r, 1, Length[planer]}, {z, 1, Length[planez]};
17 Return[intensity];];
18
19 frequency = 100000;
20 inte1 = findIntensity [frequency];
21 R = 0.0772; d = 2*0.0254; c = 340; w = 3*0.0254;
22 inte01 = Transpose[Join[Reverse[inte1], inte1]];
23 zsize = Dimensions[inte1][[2]];
24 rsize = Dimensions[inte1][[1]]*2;
25 MatrixPlot[inte01, ColorFunction -> "Rainbow",
26 FrameTicks -> { {{0, "0_cm"}, {zsize/2, "10_cm"}, {zsize, "20_cm"}},
27   Automatic}, {Automatic, {{0, -w*100/2}, {rsize/
28   4, -w*100/4}, {rsize/2, "0_cm"}, {rsize*3/4, w*100/4}, {rsize,
29   w*100/2}}}]
```

---

### A.2 Computing Fractal Dimension

Listing 2: Acoustic Phased Array simulation

---

```

1 fracDim = Function{img, t},
2   iEdge = EdgeDetect[Binarize[img, t]];
3   MinS = Floor[Min[ImageDimensions[iEdge]]/2];
4   data =
5     ParallelTable [{1/size,
6       Total[Sign /@ (Total[#, 2] & /@ (ImageData /@
7         Flatten[ImagePartition [iEdge, size ]]) )]}, {size, 10,
8       MinS/2, 10}];
9   If [Log[data], , Return []];
10  If [Element[Total[Log[data]], Reals],
11    line = Fit[Log[data], {1, x}, x], line = Null];
12  D[line, x]
13  ];
14 image = Import[f];
15 out = fracDim[image, 0.5]

```

---

## B Python code

### B.1 Generate DLA

This code generates a diffusion limited aggregate of size MAX\_PARTICLES. Code is optimized to generate a particle within a circle of a certain size slightly larger than the maximum radius of the DLA growth (given by MAX\_R). Every time MAX\_R is reached the circle increases and the rate at which particles stick decreases. On my computer 40 particles per second initially stick. For 5000 particles the code takes approximately an hour and slows to 1 particles a second.

---

```

1 #dla01.py
2
3 import numpy as np
4 import math as m
5 import random as r
6 import time
7 import matplotlib.pyplot as plt
8 from pylab import *
9 r.seed(None)
10
11 TAU=2*np.pi
12 MAX_DIM=1000
13 D2MAX=m.floor(MAX_DIM/2)

```

```

14 xym = np.matrix(np.zeros((MAX_DIM+1,MAX_DIM+1), dtype = 'bool'))
15 print_wait_time=3
16 MAX_TURNS=200000
17 MAX_PARTICLES=5150
18
19 def xy_dla(turns):
20     counter=0
21     rounds=0
22     stucknum=0
23     cnt_avg=0
24     xym[D2MAX,D2MAX]=1 #seed and centerpoint
25     #start the clock!
26     cnt_start=time.clock()
27     start_time=time.clock()
28     time_ref=time.clock()
29     print_time=time.clock()
30     cnt_avg_all=0
31     cnt_avg_succ=0
32
33     scaling_const=20
34     DIM=m.floor(MAX_DIM/scaling_const)
35     D2=m.floor((DIM/2))
36     MAX_R=np.floor(0.9*D2)-np.floor((D2/(3+m.floor(DIM/50))))
37
38     for _ in range(turns):
39         """
40         Use a circle such that a particle is placed a distance D2 from
41         the center of the plot
42         """
43         theta=r.uniform(0,TAU)
44         dis=MAX_R+((D2-MAX_R)/3)
45         pos=np.fix([ D2MAX+(dis*np.cos(theta)), D2MAX+(dis*np.sin(theta)) ])
46
47         while(True): #random drunk walk
48             direction =r.randrange(0,4,1) #0: left #1: right #2: up #3: down
49             if direction ==0: pos[0]=pos[0]-1
50             elif direction ==1: pos[0]=pos[0]+1
51             elif direction ==2: pos[1]=pos[1]+1
52             else: pos[1]=pos[1]-1
53
54             #if particle leaves our circle
55             if ((pos[0]-D2MAX)**2)+((pos[1]-D2MAX)**2)>=((1.1*dis)**2): break
56

```

```

57  #should be a better way to get the neighbors super quick for a matrix
58  #try using numpy or scipy
59  if xym[pos[0],pos [1]]: break
60  elif xym[pos[0]-1:pos[0]+2,pos[1]-1:pos[1]+2].any():
61      xym[pos[0],pos[1]]=True
62      counter = counter + 1
63      cnt_time=time.clock()-cnt_start
64      cnt_avg=(cnt_time/(counter+1))+(cnt_avg*counter/(counter+1))
65      total_time=time.clock()-start_time
66      time_ref=time.clock()
67
68  if np.amax(np.absolute(pos-D2MAX)) > MAX_R and DIM < MAX_DIM:
69      #change the size of the working radius to speed things up
70      DIM=DIM+2#m.floor(DIM + MAX_DIM/(scaling_const*2))#added DIM/
71      D2=m.floor((DIM/2))
72      #make a max close to the radius of the system
73      MAX_R=np.floor(0.9*D2)-np.floor((D2/(3+m.floor(DIM/50))))
74      if DIM >= MAX_DIM:
75          MAX_R=DIM
76          D2=m.floor(DIM/2)
77      print 'RESIZED...RESIZED...RESIZED_matrix_to_{0}'.format(DIM)
78      print '====='
79
80  if time.clock()-print_time > print_wait_time:
81      print 'Counter:_{0}_Rounds:_{1}_Hits_per_second:_{2}'.format(counter,rounds, counter/(time.
82          clock()-start_time))
83      print 'Time_taken:_{0}_Average_time_per_hit:_{1}_Total_time:_{2}'.format(cnt_time,cnt_avg,
84          total_time)
85      cnt_start=time.clock()
86      print_time=time.clock()
87      previous_hits=counter
88      print ' Position_(from_center):_{0}_Size_of_matrix:_{1}'.format(pos-D2MAX,DIM)
89      print ' Max_R:_{0}_Distance_from_center_created:_{1}'.format(MAX_R,dis)
90      print '====='
91      break
92
93  rounds = rounds+1
94  if counter > MAX_PARTICLES: break
95  LowerLimit= D2MAX-MAX_R
96  UpperLimit= D2MAX+MAX_R
97  l=np.array([LowerLimit,UpperLimit])
98  out=np.vsplit(np. hsplit (xym,l) [1], l) [1]
99  print 'Shape_of_resulting_matrix:_{0}'.format( out.shape )

```

```

98  return out
99
100 a = xy_dla(MAX_TURNS)
101 np.savetxt('dla_{0}.csv'.format(MAX_PARTICLES), a, delimiter=",",fmt='%i')
102 file_nm='dla_{0}.png'.format(MAX_PARTICLES)
103 plt.savefig(file_nm)
104
105 # now get a list of points where the particles stuck and save them.
106 # Seed is in origin so shift everything by D2MAX
107 xyl=np.array([0,0], dtype=np.dtype('>i4'))
108 x_center=m.floor(a.shape[0]/2)
109 y_center=m.floor(a.shape[1]/2)
110 for i in range(0,a.shape[0]):
111     for j in range(0,a.shape[1]):
112         if a[i,j]==True:
113             xyl=np.vstack((xyl,np.array([i-x_center,j-y_center])))
114
115 np.savetxt('dla_{0}_points.csv'.format(MAX_PARTICLES), xyl, delimiter=",", fmt='%i')
116 plt.plot(xyl[:,0], xyl[:,1], 'ro')
117 plt.axis([-x_center, x_center, -y_center, y_center])
118 plt.savefig(file_nm)
119 plt.show()

```

---

## C Evaporation Notes

Pressure is in Torr. Amperage is in Amps (AC).  $\uparrow$  means scaling up entry during time period stated. All runs are measured using the Terranova 907 controller with a convection gauge. Max vacuum by belt pump determined to be under 40mTorr in all cases. All runs, unless explicitly stated, are vented with 99.999% Argon until vacuum gauge reads under 40mTorr on the "Arg" setting. Boats were naively chosen based on size of pellets and using a deposition chart. All boat types are listed.

### C.1 6/09/12, Cu-black

Copper black evaporation. No water cooling. One of the initial test runs to determine how the evaporation setup should be set up. Used Molybdenum boat (Rdmathis S2B-AO-Mo). Substrate is glass cover slide. Distance is 10cm.

Time	P $\pm$ variation	A $\pm$ variation	Notes
10 : 40	$0.860 \pm 0.05$	$\uparrow 140 \pm 3$	Ramped up current
31 : 05	$0.820 \pm 0.03$	$\uparrow 180 \pm 4$	Ramped up current
1 : 00 : 00	$0.820 \pm 0.03$	180	Started shut-off
1 : 02 : 00	$0.800 \pm 0.03$	0	Shut-off complete

Notes: Created Copper black that was not dark at all. Coloration was slight to none. Assume that water cooling is needed.

## C.2 7/03/12, Cu-black

Data not recorded, only sample remains. Sample has copper leads and tin foil wrapped around edges. The result is some non-consistent black spread around foil and copper.

## C.3 7/11/12, Cu-black

Water cooling setup as shown in Figure 1(a). Will try to keep pressure between 800 and 900 mTorr. Used Molybdenum boat (Rdmathis S2B-AO-Mo). Substrate is glass cover slide. Distance is 10cm.

Time	P $\pm$ variation	A $\pm$ variation	Notes
18 : 22	$0.880 \pm 0.05$	$\uparrow 165 \pm 5$	Ramped up current until Cu melted
26 : 03	$0.820 \pm 0.02$	$\uparrow 180 \pm 4$	Ramped up current, Cu-black appears
31 : 04	$0.860 \pm 0.03$	180	Thick layer reported. Started shut-off
37 : 07	$0.880 \pm 0.03$	$\downarrow 0$	Shut-off complete
1 : 08 : 14	$0.743 \pm 0.05$	0	Started vent after cool-down

Notes: Substrate 1: Glass slide with copper "leads". No deposits visible on glass, some dark green deposits visible on copper leads.

Created Copper black that was not very dark and similar to Copper without cooling. Assume that the pressure is not high enough to create enough heat transfer to the substrate that the films will not melt. Next run should be in the 2.5Torr range.

## C.4 7/12/12, In-black

Water cooling setup as shown in Figure 1(a). Working pressure is  $1.05 \pm 0.05$ Torr. Used Molybdenum boat (Rdmathis S2B-AO-Mo). Substrate is glass cover slide. Distance is 15cm.

Time	P $\pm$ variation	A $\pm$ variation	Notes
10 : 50	1.05 $\pm$ 0.05	$\uparrow$ 125.5 $\pm$ 0.4	Current up. In already melted
15 : 11	1.05 $\pm$ 0.05	$\uparrow$ 135.4 $\pm$ 1.0	Current up. In slow evaporation
20 : 50	1.05 $\pm$ 0.05	$\uparrow$ 145.0 $\pm$ 1.0	Current up. In evaporation
27 : 41	1.05 $\pm$ 0.05	145.0 $\pm$ 1.0	Thick film seems to have developed
57 : 45	1.05 $\pm$ 0.05	148.0 $\pm$ 2.0	Current has become more erratic. Shut-down
58 : 08	1.05 $\pm$ 0.05	0	Stopped
1 : 10 : 40	0.944 $\pm$ 0.03	0	Cool down complete

Notes: Indium in the boat has been used up completely. Indium is grey and not black. Idea is to use less time to reduce the heat.

Substrate 1: Indium is on copper leads and somewhat on glass slide. Growth seems to be originating from the center and growing outwards on the glass part. Copper part has Indium uniformly spread except for edges where the indium suddenly thins out.

### C.5 7/13/12, In-black

Water cooling setup as shown in Figure 1(a). Working pressure is 2.00 $\pm$ 0.10Torr. Used Molybdenum boat (Rdmathis S2B-AO-Mo). Substrate is glass cover slide. Distance is 15cm.

Time	P $\pm$ variation	A $\pm$ variation	Notes
12 : 30	2.00 $\pm$ 0.05	$\uparrow$ 120 $\pm$ 1.0	Current up. In already melted
55 : 00	2.00 $\pm$ 0.05	$\uparrow$ 155 $\pm$ 2.0	Current up. In evaporating
59 : 30	2.00 $\pm$ 0.05	155 $\pm$ 2.0	Shutting off

Notes: Not all Indium used. The Indium is about the same shade of grey as before. Seems that Indium will always be a shade of grey.

Substrate 1: Glass slide is successfully covered with grey indium. Has uniform distribution except where there were holes in the substrate holder. There is slight transparency in those places. Seems to imply that a free hanging glass slide would not have a good deposition.

### C.6 7/13/12, Al-black

Water cooling setup as shown in Figure 1(a). Working pressure is 2.00 $\pm$ 0.10Torr. Used Tungsten boat (Rdmathis S38-.010W). Substrate is glass cover slide. Distance is 15cm. Using aluminum pieces that are quite large.



Time	P $\pm$ variation	A $\pm$ variation	Notes
52 : 52	2.00 $\pm$ 0.05	$\uparrow$ 230 $\pm$ 4.0	Current up. Al not melting
53 : 18	2.00 $\pm$ 0.05	0	SCR turned itself off

Notes: Aluminum did not melt. Developed a matte film around itself. Later tried another run by ramping up to 220 amps in 15:20 and adding another aluminum pellet. New pellet melted first, then old pellet “crumpled” into a ball. Current on the order of 200 amps was run until SCR turned itself off after over half an hour. Result were a thin grey film around evaporator that shorted the leads from the SCR. Substrates had a shiny grey hue on one side and were mirrors on the other leading to speculation that the aluminum melted and wetted the substrates. Leads in the evaporator had to be cleaned after deposition after being shorted by the aluminum.

Substrate from second run: Result is almost completely uniform grey Aluminum with transparency where the holes were on the substrate holder, shininess on one side, and mirror on the other.

### C.7 7/17/12, Al-black

Water cooling setup as shown in Figure 1(a). Working pressure is 2.00 $\pm$ 0.10Torr. Used Tungsten boat (Rdmathis S38-.010W). Substrate is glass cover slide. Distance is 15cm. Using aluminum pieces that are sawed off.

Time	P $\pm$ variation	A $\pm$ variation	Notes
24 : 26	2.00 $\pm$ 0.05	$\uparrow$ 212.1 $\pm$ 4.0	Current up. Al melted
25 : 35	2.50 $\pm$ 0.20	$\downarrow$ 200.1 $\pm$ 4.0	Current down
34 : 21	2.50 $\pm$ 0.20	200.0 $\pm$ 4.0	Seeing some brown deposits
39 : 45	2.50 $\pm$ 0.20	0	Boat broke

Notes: Lowered current in the middle of the evaporation since Al has better thermal contact. Boat broke after 3 minutes 40 seconds of depositing. Received great results. Aluminum deposited was black. The deposition ranges from very dark to slightly less dark and more reflective along the substrate. Seems to imply that even though there is a large distance between the substrate and source there are portions that receive better deposition related to distance.

### C.8 7/17/12, Al-black

Water cooling setup as shown in Figure 1(a). Working pressure is 2.00 $\pm$ 0.10Torr. Used Tungsten boat (Rdmathis S38-.010W). Substrate is glass cover slide. Distance is 15cm.

Using aluminum pieces that are sawed off and pre-melted from previous aluminum run.

Time	P $\pm$ variation	A $\pm$ variation	Notes
15 : 59	$2.00 \pm 0.10$	$\uparrow 130 \pm 2.0$	Current up. Al melted?
20 : 21	$2.50 \pm 0.20$	$\uparrow 140 \pm 3.0$	Current up, fog appears on mirror
45 : 57	$2.50 \pm 0.20$	$140 \pm 3.0$	
46 : 22	$2.50 \pm 0.20$	$\downarrow 0$	Stopping

Notes: No real results. A very thin coating covers some substrates. Extremely low current for this deposition are not fully understood.

### C.9 7/17/12, In-black

Water cooling setup as shown in Figure 1(a). Working pressure is  $5.00 \pm 0.20$ Torr. Used Molybdenum boat (Rdmathis S2B-AO-Mo). Substrate is glass cover slide. Distance is 15cm.

Time	P $\pm$ variation	A $\pm$ variation	Notes
14 : 11	$5.25 \pm 0.20$	$\uparrow 140.5 \pm 1.0$	Current up. Started Dep.
54 : 04	$5.25 \pm 0.20$	$140.0 \pm 1.0$	long deposition
1 : 11 : 56	$4.40 \pm 0.10$	0	Cool down

Deposited Indium at 140 amps and 5Torr vacuum for 40 minutes. Result was slightly different than previous grey Indium.

Substrate 1: Glass slide with lightly colored holes where substrate holder has holes. Results is obviously darker than previous Indium evaporation when examined side-by-side. Growth seems to also be much more uniform than previous depositions of Indium.

### C.10 7/17/12, Cu-black

Water cooling setup as shown in Figure 1(a). Working pressure is  $5.00 \pm 0.50$ Torr. Used Molybdenum boat (Rdmathis S2B-AO-Mo). Substrate is glass cover slide. Distance is 15cm.

Time	P $\pm$ variation	A $\pm$ variation	Notes
10 : 50	$5.15 \pm 0.20$	$\uparrow 150.1 \pm 1.0$	Cu melted
38 : 51	$5.15 \pm 0.30$	$\uparrow 190 \pm 1.0$	Getting black
49 : 33	$5.15 \pm 0.50$	0	Ended deposition

Deposited Copper at 190 amps and 5.50 Torr for 11:51.

### C.11 7/19/12, Cu-black

Water cooling setup as shown in Figure 1(a). Working pressure is  $5.00 \pm 0.20$  Torr. Used Molybdenum boat (Rdmathis S2B-AO-Mo). Substrate is glass cover slide. Distance is 15cm.

Time	P $\pm$ variation	A $\pm$ variation	Notes
19 : 57	$5.00 \pm 0.20$	$\uparrow 180.4 \pm 2.0$	Current up
22 : 57	$5.00 \pm 0.50$	$179.4 \pm 2.0$	Deposition started
42 : 49	$5.00 \pm 0.50$	0	Ended deposition
1 : 01 : 37	$5.00 \pm 0.3$	0	Opening bell jar

Substrate 1: Glass slide with copper wetting layer on two ends. Thin layer of whitish copper deposited uniformly on substrate in contrast to previous runs where copper only adhered to the copper layer.

### C.12 7/19/12, Al-black

Water cooling setup as shown in Figure 1(a). Working pressure is  $4.50 \pm 0.50$  Torr. Used Tungsten boat (Rdmathis S38-.010W). Substrate is glass cover slide. Distance is 15cm. Using aluminum pieces that are sawed off.

Time	P $\pm$ variation	A $\pm$ variation	Notes
20 : 52	$5.00 \pm 0.60$	$\uparrow 184.1 \pm 2.0$	Current up, Al melted
30 : 53	$5.00 \pm 0.90$	$\uparrow 194.4 \pm 3.0$	Current up, waiting for dep
34 : 15	$5.00 \pm 0.90$	0	boat broke

No results to show.

### C.13 7/19/12, Cu-black

Water cooling setup as shown in Figure 1(a). Working pressure is  $5.00 \pm 0.20$  Torr. Used Molybdenum boat (Rdmathis S2B-AO-Mo). Substrate is glass cover slide. Distance is 15cm.

Time	P $\pm$ variation	A $\pm$ variation	Notes
19 : 04	$5.00 \pm 0.20$	$\uparrow 176.6 \pm 2.0$	Current up, Cu melted
27 : 51	$5.00 \pm 0.20$	$\uparrow 179.1 \pm 2.0$	Current up, waiting for dep
2 : 16 : 12	$5.00 \pm 0.90$	0	very long dep

Very long deposition of Cu. Started becoming difficult to control pressure, went as high as 8 Torr. Obtained poor results.

### C.14 7/20/12, Cu-black

Water cooling setup as shown in Figure 1(a). Working pressure is  $5.00 \pm 0.20$  Torr. Used Molybdenum boat (Rdmathis S2B-AO-Mo). Substrate is glass cover slide. Distance is 15cm. Unique run in that slowly increase current until melt and then slowly decrease.

Time	P $\pm$ variation	A $\pm$ variation	Notes
1 : 27	$4.30 \pm 0.10$	0	Start current up
1 : 53	$4.30 \pm 0.20$	$\uparrow 179.1 \pm 2.0$	Current up, waiting for dep
1 : 57	$4.30 \pm 0.30$	$\downarrow 165 \pm 2.0$	Slowly lowering Current
2 : 13	$4.50 \pm 0.20$	$\downarrow 0$	Lowered current to 0

Substrate 1: Glass slide with copper wetting layer on edges. Has uniform black deposit along substrate. Deposit has tints of brown in it.

### C.15 7/23/12, Al-black

Water cooling setup as shown in Figure 1(a). Working pressure is  $4.50 \pm 0.50$  Torr. Used Tungsten boat (Rdmathis S38-.010W). Substrate is glass cover slide. Distance is 15cm. Using aluminum pieces that are sawed off.

Time	P $\pm$ variation	A $\pm$ variation	Notes
21 : 40	$4.00 \pm 0.30$	$\uparrow 204.6$	Current up
38 : 46	$4.00 \pm 0.50$	$\uparrow 207.6 \pm 4.0$	Current up, waiting for dep
45 : 55	$4.00 \pm 0.60$	$210.4 \pm 2.0$	Some grey deposition
51 : 06	$4.50 \pm 0.60$	$\downarrow 0$	No more dep seen

Gray films everywhere. Poor deposition.

### C.16 7/23/12, Al-black

Water cooling setup as shown in Figure 1(a). Working pressure is  $5.00 \pm 0.50$  Torr. Used Tungsten boat (Rdmathis S38-.010W). Substrate is glass cover slide. Distance is 15cm. Using aluminum pieces that are sawed off.

Time	P $\pm$ variation	A $\pm$ variation	Notes
13 : 04	$5.00 \pm 0.50$	$\uparrow 213.2$	Current up, Al melted
15 : 21	$5.00 \pm 0.50$	209.2	Ending dep, mirror is darkened.

### C.17 7/24/13, In-black

Water cooling setup as shown in Figure 1(a). Working pressure is  $4.00 \pm 0.20$  Torr. Used Molybdenum boat (Rdmathis S2B-AO-Mo). Substrate is glass cover slide. Distance is 15cm.

Time	P $\pm$ variation	A $\pm$ variation	Notes
10 : 17	$4.00 \pm 0.20$	$\uparrow 134.2$	Current up, In evaporating
13 : 40	$4.00 \pm 0.20$	134.3	Deposition.
16 : 50	$4.00 \pm 0.20$	0	Lowered current to 0

Started a new deposition by venting to room pressure and then back down to 4 Torr.

Time	P $\pm$ variation	A $\pm$ variation	Notes
0	$4.00 \pm 0.20$	0	Start
13 : 10	$4.00 \pm 0.20$	$\uparrow 134.5$	Deposition.
13 : 20	$4.00 \pm 0.20$	$\downarrow 0$	Lowered current to 0
20 : 46	$4.00 \pm 0.20$	0	Starting increase again
23 : 52	$4.00 \pm 0.20$	$\uparrow 136.5$	Current up
33 : 22	$4.00 \pm 0.30$	134.2	Start shut down

### C.18 7/25/12, In-black

Water cooling setup as shown in Figure 1(a). Working pressure is  $5.00 \pm 0.20$  Torr. Used Molybdenum boat (Rdmathis S2B-AO-Mo). Substrate is glass cover slide. Distance is 15cm.

Unique run where pressure was kept around 4.00 Torr. SCR was turned up to 140 Amps 3 times over an hour. Logs were not kept since the viewfinder was used to judge heat and deposition time.

Produced very uniform distribution of indium grey the same shade as dark indium deposited on 07/17/2012. Substrates were glass slides with wetting copper layers on the edges.

Other substrates include tin foil with similar deposition and the mirror substrate with a darker despite than all the other substrates. Mirror substrate had gradient towards center where the deposit is lighter.

### C.19 8/03/12, Al-black

Water cooling setup as shown in Figure 1(a). Working pressure is 5.00. Used Molybdenum boat (Rdmathis S2B-AO-Mo). Substrate is glass cover slide. Distance is 15cm.

Time	P $\pm$ variation	A $\pm$ variation	Notes
6 : 00	4.00 $\pm$ 0.30	$\uparrow$ 99	Boat begins to glow
25 : 15	4.00 $\pm$ 0.40	$\uparrow$ 175	Aluminum liquified, lower current
26 : 06	4.00 $\pm$ 0.50	$\downarrow$ 170	
38 : 36	4.00 $\pm$ 0.50	$\uparrow$ 200	
48 : 16	4.00 $\pm$ 0.60	200	Start shutdown

Produced blue coating on tin foil surrounding substrates. Mirror substrate was a light blue color as well.

### C.20 8/03/12, Al-black

Water cooling setup as shown in Figure 1(a). Working pressure is 5.00. Used Molybdenum boat (Rdmathis S2B-AO-Mo). Substrate is glass cover slide. Distance is 15cm.

Used same piece of aluminum as last run. Boat was found to be suddenly broken.

### C.21 8/06/12, In-black

Water cooling setup as shown in Figure 1(a). Working pressure is 4.00. Used Tungsten boat (Rdmathis S2B-.010W). Substrate is glass cover slide. Distance is 15cm.

Boat is now Tungsten with no Aluminum Oxide coating.

Time	P $\pm$ variation	A $\pm$ variation	Notes
15 : 49	4.00 $\pm$ 0.20	$\uparrow$ 130	Depositing
23 : 17	4.00 $\pm$ 0.20	$\downarrow$ 0	Waiting for 30 minutes
56 : 53	4.00 $\pm$ 0.20	$\uparrow$ 130	Depositing
1 : 23 : 10	4.00 $\pm$ 0.20	$\downarrow$ 0	Waiting for 9 minutes
1 : 34 : 46	4.00 $\pm$ 0.20	$\uparrow$ 130	Depositing
1 : 36 : 03	4.00 $\pm$ 0.20	$\downarrow$ 0	Stopping

Results are the darkest ever received for Indium. Samples remained a very dark grey (but do not appear black under the human eye).

### C.22 8/06/12, Al-black

Water cooling setup as shown in Figure 1(a). Working pressure is 2.00. Used Tungsten boat (Rdmathis S2B-.010W). Substrate is glass cover slide. Distance is 15cm.

Time	P $\pm$ variation	A $\pm$ variation	Notes
15 : 35	$2.00 \pm 0.40$	$\uparrow 172.8$	Liquified
30 : 15	$2.00 \pm 0.60$	$\uparrow 217$	SCR shut itself off

No results. The SCR shut itself off and there was deposition to be seen. Tried again with the same settings and SCR turns itself off at 220amps.

### C.23 8/07/12, Sn-black

Water cooling setup as shown in Figure 1(a). Working pressure is 3.50. Used Molybdenum boat (Rdmathis S2B-AO-Mo). Substrate is glass cover slide. Distance is 15cm. Transformer switch to 1st setting.

Per deposition notes Sn needs slightly higher current than Cu.

Time	P $\pm$ variation	A $\pm$ variation	Notes
6 : 32	$3.50 \pm 0.30$	$\uparrow 112$	Liquified
20 : 23	$3.50 \pm 0.50$	$\uparrow 175$	Slow evaporation started
41 : 04	$3.50 \pm 0.50$	$\downarrow 0$	Started shutoff
1 : 12 : 56	$3.50 \pm -0.50$	0	Cooled and vented

Poor results. Very thin layer of transparent Sn was deposited.

### C.24 8/08/12, Cu-black

Water cooling setup as shown in Figure 1(a). Working pressure is 4.50. Used Molybdenum boat (Rdmathis S2B-.010Mo). Substrate is thin Mica. Distance is 15cm.

Time	P $\pm$ variation	A $\pm$ variation	Notes
6 : 29	$4.50 \pm 0.30$	$\uparrow 170$	Depositing
9 : 20	$4.50 \pm 0.30$	$\downarrow 0$	SCR down temporarily
21 : 02	$4.50 \pm 0.30$	$\uparrow 165$	Depositing
25 : 47	$4.50 \pm 0.30$	$\downarrow 0$	Shut-off

Results were very good. Copper held on Mica well.

### C.25 8/09/12, Mg-black

Water cooling setup as shown in Figure 1(a). Working pressure is 4.50. Used Molybdenum boat (Rdmathis S1-.005Mo). Substrate is thin Mica. Distance is 15cm.

Used magnesium piece from camping flint.

Time	P $\pm$ variation	A $\pm$ variation	Notes
10 : 24	$4.50 \pm 0.30$	$\uparrow 140$	Depositing
22 : 00	$4.50 \pm 0.30$	0	Shutdown

Results was very white with black edges. Could potentially get black Magnesium based on black portions of films but decided not to based on low number of possible applications.

### C.26 8/24/12, Cr-black

Water cooling setup as shown in Figure 1(a). Working pressure is 3.00. Used Chromium covered filament for deposition.

Time	P $\pm$ variation	A $\pm$ variation	Notes
9 : 24	$3.00 \pm 0.30$	$\uparrow 120$	Despositing
16 : 10	$3.00 \pm 0.40$	120	Depositing

After 16 : 10 time a valve was accidentally opened to room pressure and the bell jar started becoming foggy. Smoke appeared and showed convection currents. Different types of deposits appeared on the walls.

Results were of course not ideal due to the presence of air. This run produced interesting patterns on most surfaces around the evaporator. Most films were grey with green “veins”. Chromium Oxide is green and the most likely candidate for the green results on the films.

### C.27 8/31/12, Au-black

Water cooling setup as shown in Figure 1(a). Working pressure is 4.50. Used Molybdenum boat with alumina oxide coating (Rdmathis S2B-AO-Mo). Substrate is glass cover slides and many hanging pieces of foil at various distances. Farthest distance is 15cm. Transformer initially on '9'.

Time	P $\pm$ variation	A $\pm$ variation	Notes
7 : 28	$4.50 \pm 0.20$	$\uparrow 113 \pm 2$	Reached incandescence
10 : 39	$4.50 \pm 0.30$	$\uparrow 161 \pm 2$	Melted
12 : 29	$4.50 \pm 0.30$	$\downarrow\downarrow 0$	SCR shut itself off
13 : 52	$4.50 \pm 0.20$	0	Changed SCR to '7'
14 : 58	$4.50 \pm 0.20$	0	Starting again
22 : 30	$4.50 \pm 0.40$	$\uparrow 180 \pm 5$	Some black depositing
27 : 30	$4.50 \pm 0.60$	$\uparrow 205 \pm 7$	Mirror appears black
29 : 29	$4.50 \pm 0.60$	$\downarrow\downarrow 0$	SCR shut itself off



Results: Most substrates received poor results except some foil near the boat source, mica film on the cooled plate, and the mirror substrate. Most glass substrates have a purple tint due to gold black. The mirror substrate has purple film on the edges that slowly turns black towards the middle and is one of the best deposition. Next best is mica a distance 1 inch away from the boat source that has a black spot 8mm by 5mm with the rest of the sample covered in dark grey film. Copper foil hanging 1.5 inches away has dark deposits that slowly turn grey the farther the portion of foil is away from the source. Next are covered for the electric leads supporting the boat. These did not have direct line-of-sight to the boat but developed a dark film that fades to light brown. One of these samples has thin-film interference patterns all over it and was considerably more crumpled than the other. Distances of the “electric lead” samples were between 2 and 5 inches with closest region receiving the best results. All other films received poor results if they were more than 3 inches away from the boat source.

### C.28 9/06/12, Fe-black

Water cooling setup as shown in Figure 1(a). Working pressure is 4.50. Used Tungsten boat with high resistance (Rdmathis S3-.010W). Substrate is glass slides. Distance is 15cm.

Time	P $\pm$ variation	A $\pm$ variation	Notes
10 : 13	4.50 $\pm$ 0.30	$\uparrow$ 180 $\pm$ 2	Iron melted
14 : 29	4.50 $\pm$ 0.40	$\uparrow$ 195 $\pm$ 3	Watching
20 : 29	4.50 $\pm$ 0.40	$\downarrow$ 0	SCR off

Results: Poor deposition on substrates. Mirror substrate had best deposition: very black toward center that thins out to a faint brown color.

### C.29 9/10/12, Fe-black

Water cooling setup as shown in Figure 1(a). Working pressure is 4.00. Unique substrate “holder” using copper foil with cut-out pieces facing normal to the boat source. The attempt is made to find the correlation between distance and thickness of films while having a uniform distribution on as many substrates as possible.

Time	P $\pm$ variation	A $\pm$ variation	Notes
10 : 35	4.00 $\pm$ 0.50	$\uparrow$ 215 $\pm$ 6	Iron melted
35 : 30	4.00 $\pm$ 0.60	$\uparrow$ 230 $\pm$ 6	Starting shut-down
36 : 07	4.00 $\pm$ 0.60	$\downarrow$ 0	done

Results: Determined that angle does not seem to play an important role in deposition. Instead position and distance play a much greater role in the darkness of the films. Two samples produced very dark and black films: one that was 2 inches away and another than was 3 inches away. Farther samples did not have any sample adhere at all. Black spots faded to light brown.

### C.30 2/14/13, Cu-black

Water cooling setup as shown in Figure 1(a). Working pressure is 3.50. Used Tungsten boat (Rdmathis S2B-.010W). Copper foil overhanging. Distance is 7cm.

Time	P $\pm$ variation	A $\pm$ variation	Notes
1 : 00	3.50 $\pm$ 0.30	$\uparrow$ 180 $\pm$ 4(65%)	Raised current
5 : 58	3.50 $\pm$ 0.50	180 $\pm$ 3	Start shut-off

Notes: 6 minutes deposition resulted in the greatest black copper deposition as apparent the human eye. This copper sample corresponds to the darkest reflectance shown above. Texture of the sample appear very “velvety” and tapers off with distance into an array of visible black clumps much like dust. A thin coating of transparent dark green film continues on the substrate. Velvet appearance is continuous from 7cm distance to 9cm distance. Clumps appear from 9cm to 11cm away, and the thin film continues up to 14 cm away past line-of-sight of the source.

### C.31 4/05/13,Cu-black

New water cooling setup as shown in Figure 1(b). Working pressure is 5.00. Used Tungsten boat with alumina oxide coating (Rdmathis S2B-AO-W). Substrate is rounded watch-glass camped down onto cooler.

Time	P $\pm$ variation	A $\pm$ variation	Notes
7 : 13	5.00 $\pm$ 0.30	$\uparrow$ 153 $\pm$ 3	Copper melted
19 : 12	5.00 $\pm$ 0.50	$\uparrow$ 170 $\pm$ 5	Depositing
28 : 15	5.00 $\pm$ 0.60	$\downarrow\downarrow$ 0	Boat broke

Found that the watch glass broke mid-run and melted onto the boat causing it to break. The heating of the glass probably caused it to shatter and it was difficult to see due to the heat transfer into the large pieces of glass touching the boat. Run was a failure but will try again.

### C.32 4/15/13, Cu-black

New water cooling setup as shown in Figure 1(b). Working pressure is 5.00 Torr. Used Tungsten boat (Rdmathis S2B-.010W). Substrate is rounded watch-glass camped down onto cooler.

Time	P $\pm$ variation	A $\pm$ variation	Notes
11 : 28	5.00 $\pm$ 0.50	$\uparrow$ 170 $\pm$ 4	Depositing
18 : 13	5.00 $\pm$ 0.50	170 $\pm$ 4	shutting down

Produced a non-uniform distribution of black copper film on the watch glass. The center, with a radius approximately 5cm, is black and all other parts of the watch glass is a light transparent color. The mirror substrate is very black but, like the previous deposition onto copper foil, has “clumps” of black copper scatters around the area father from the source.

### C.33 4/29/13, Cu-black

New water cooling setup as shown in Figure 1(b). Working pressure is 1.00 Torr. Used Tungsten boat (Rdmathis S2B-.010W). Substrate is copper foil tied down to cooled copper plate.

Time	P $\pm$ variation	A $\pm$ variation	Notes
13 : 42	1.00 $\pm$ 0.40	$\uparrow$ 45%	Depositing
18 : 17	1.00 $\pm$ 0.40	$\downarrow$ 0	Shutting off

Produced a good black film that turns somewhat transparent over time. The body of the film is now a dull transparent color with some small black portions.

### C.34 5/03/13, Sn-black

New water cooling setup as shown in Figure 1(b). Working pressure is 5.00. Used Molybdenum (Rdmathis S2B-.010M). Substrate is copper foil tied down to cooled copper plate.

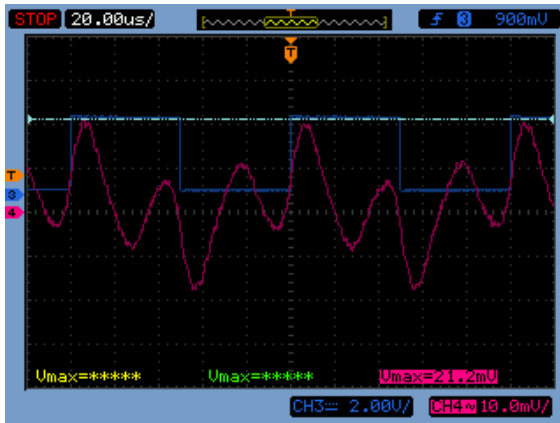
Time	P $\pm$ variation	A $\pm$ variation	Notes
24 : 04	5.00 $\pm$ 0.40	$\uparrow$ 180	Depositing
31 : 21	5.00 $\pm$ 0.50	180	Shutting down

Result was a very good deposition of Tin with some shininess on it in the center between the holders. Over time the sample turns transparent except for a free-hanging edge about 7cm away.

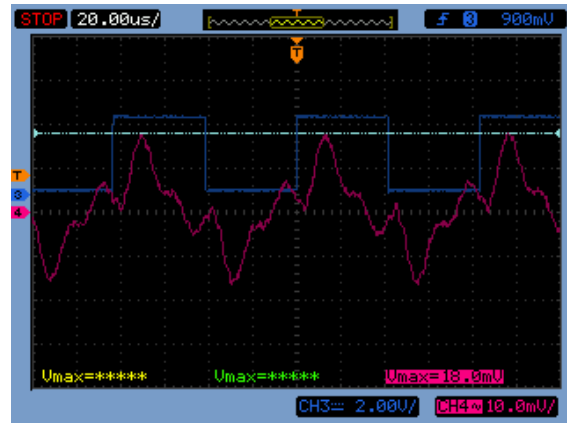
## D Photoacoustic data

The following pictures are screenshots on an oscilloscope from a MEMs microphone measuring the photoacoustic signal from a copper black film with a 671nm pulsing laser incident on the film. In order to get the loudest results the film and microphone are facing directly towards each other. Input waveform was a 50% duty cycle square wave:

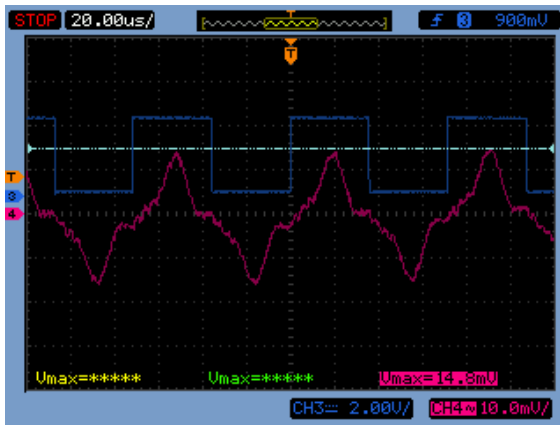
10kHz



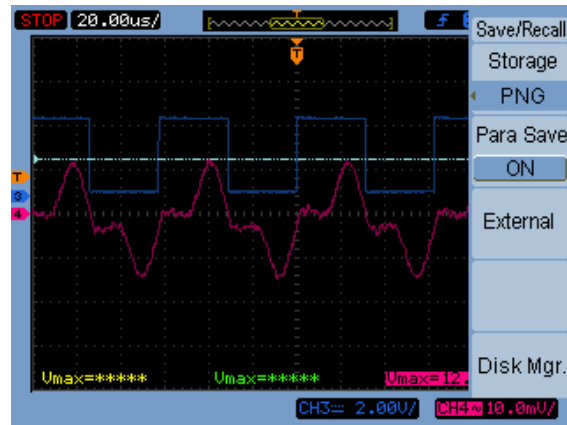
12kHz



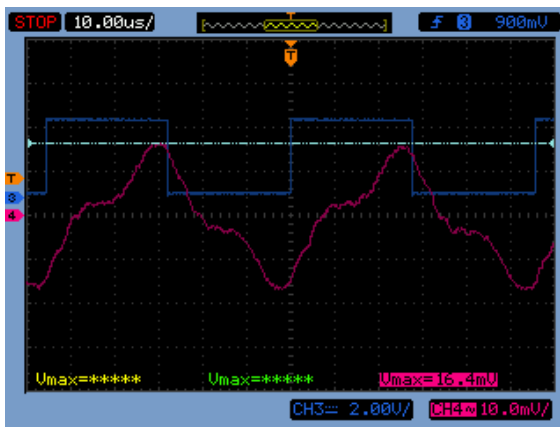
14kHz



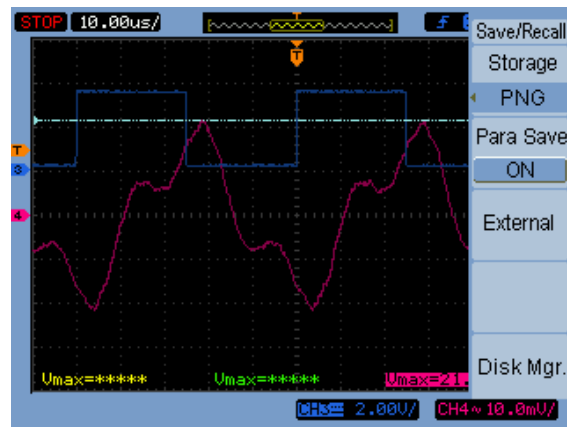
16kHz



18kHz

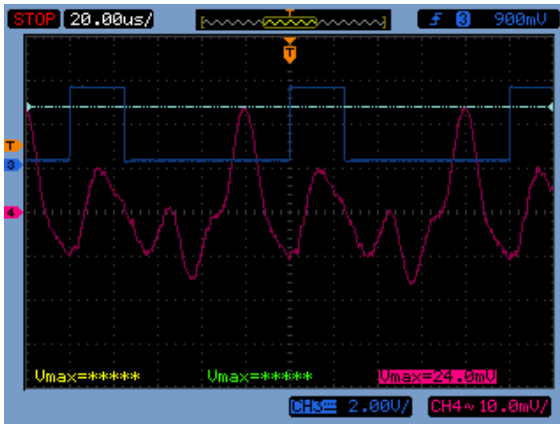


20kHz

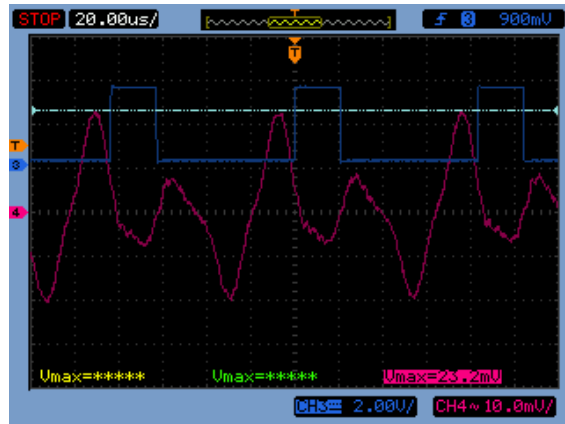


Input waveform with a 25% duty cycle square wave:

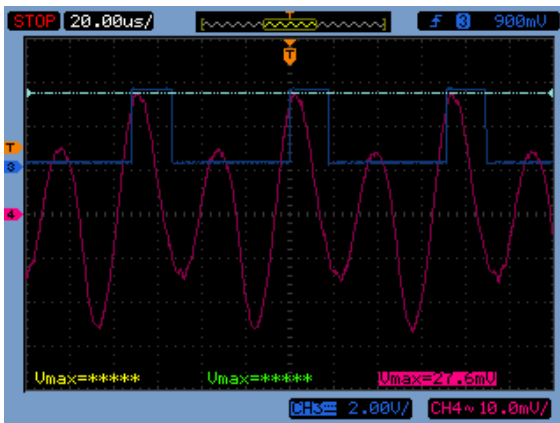
10kHz



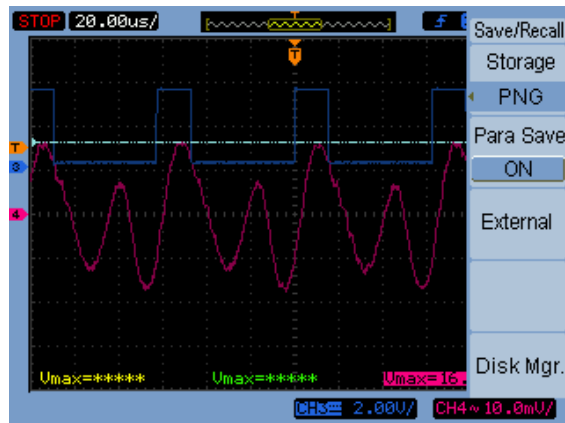
12kHz



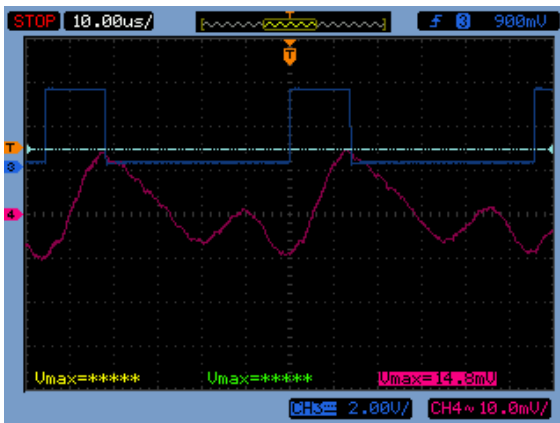
14kHz



16kHz



18kHz



20kHz



## References

- [1] *275 series Convection Vacuum Gauge User Manual*. [http://www.lesker.com/NewWeb/Gauges/pdf/manuals/KJLC\\_275\\_Series\\_manual\\_v103.pdf](http://www.lesker.com/NewWeb/Gauges/pdf/manuals/KJLC_275_Series_manual_v103.pdf); Last accessed: 05/16/13.
- [2] A. G. Bell. “On the Production and Reproduction of Sound by Light”. In: *American Journal of Sciences* XX.118 (Oct. 1880), pp. 305–324.
- [3] James B. Gillespie, James D. Lindberg, and Larry S. Laude. “Kubelka-Munk Optical Coefficients for a Barium Sulfate White Reflectance Standard”. In: *Appl. Opt.* 14.4 (Apr. 1975), pp. 807–809. DOI: [10.1364/AO.14.000807](https://doi.org/10.1364/AO.14.000807).
- [4] Louis Harris, Rosemary T. McGinnies, and Benjamin M. Siegel. “The Preparation and Optical Properties of Gold Blacks”. In: *J. Opt. Soc. Am.* 38.7 (July 1948), pp. 582–588. DOI: [10.1364/JOSA.38.000582](https://doi.org/10.1364/JOSA.38.000582).
- [5] P. Jensen et al. “A fractal model for the first stages of thin film growth”. In: *Fractals* 4.3 (Oct. 1995), pp. 321–329.
- [6] *Kaye and Laby Tables of Physical and Chemical Constants*. [http://www.kayelaby.npl.co.uk/chemistry/3\\_4/3\\_4\\_4.html](http://www.kayelaby.npl.co.uk/chemistry/3_4/3_4_4.html); Last accessed: 05/16/13.
- [7] Nick Knighton and Bruce Bugbee. *A Mixture of barium sulfate and white paint*. Online.
- [8] John Lehman et al. “Gold-black coatings for freestanding pyroelectric detectors”. In: *Measurement Science and Technology* 14.7 (2003), p. 916.
- [9] E. M. Patterson, C. E. Shelden, and B. H. Stockton. “Kubelka-Munk optical properties of a barium sulfate white reflectance standard”. In: *Appl. Opt.* 16.3 (Mar. 1977), pp. 729–732. DOI: [10.1364/AO.16.000729](https://doi.org/10.1364/AO.16.000729).
- [10] A. Rosencwaig. *Photoacoustics and photoacoustic spectroscopy*. Chemical analysis. Wiley, 1980. ISBN: 9780471044956.
- [11] Allan Rosencwaig and Allen Gersho. “Theory of the photoacoustic effect with solids”. In: *Journal of Applied Physics* 47.1 (1976), pp. 64–69. DOI: [10.1063/1.322296](https://doi.org/10.1063/1.322296).
- [12] C.-M. Wang et al. “Microstructure and Absorption Property of Silver-Black Coatings”. In: *Japanese Journal of Applied Physics* 39 (Feb. 2000), p. 551. DOI: [10.1143/JJAP.39.551](https://doi.org/10.1143/JJAP.39.551).